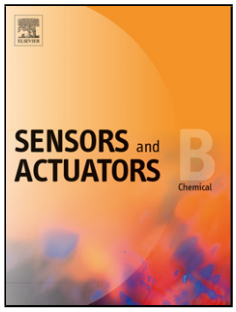

Title: Spheroids-on-a-chip: Recent advances and design considerations in microfluidic platforms for spheroid formation and culture

Authors: Khashayar Moshksayan, Navid Kashaninejad, Majid Ebrahimi Warkiani, John G. Lock, Hajar Moghadas, Bahar Firoozabadi, Mohammad Said Saidi, Nam-Trung Nguyen

PII: S0925-4005(18)30248-X
DOI: https://doi.org/10.1016/j.snb.2018.01.223
Reference: SNB 24072

To appear in: *Sensors and Actuators B*

Received date: 31-10-2017
Revised date: 13-1-2018
Accepted date: 29-1-2018

Please cite this article as: Khashayar Moshksayan, Navid Kashaninejad, Majid Ebrahimi Warkiani, John G.Lock, Hajar Moghadas, Bahar Firoozabadi, Mohammad Said Saidi, Nam-Trung Nguyen, Spheroids-on-a-chip: Recent advances and design considerations in microfluidic platforms for spheroid formation and culture, Sensors and Actuators B: Chemical https://doi.org/10.1016/j.snb.2018.01.223

Spheroids-on-a-chip: Recent advances and design considerations in microfluidic platforms for spheroid formation and culture

Khashayar Moshksayan,[a] Navid Kashaninejad, [b] Majid Ebrahimi Warkiani, [c] John G. Lock, [d] Hajar Moghadas, [a] Bahar Firoozabadi, [a] Mohammad Said Saidi, [a, *] and Nam-Trung Nguyen [b, *]

[a] *School of Mechanical Engineering, Sharif University of Technology, 11155-9567, Iran*
[b] *Queensland Micro- and Nanotechnology Centre, Griffith University, QLD 4111, Australia*
[c] *School of Biomedical Engineering, University of Technology Sydney, NSW 2007, Australia*
[d] *University of New South Wales, EMBL Australia Node in Single Molecule Science, School of Medical Sciences, and ARC Centre of Excellence in Advanced Molecular Imaging, NSW 2052, Australia*

[*] Corresponding author1. Tel.: +98 216 616 5558 ; e-mail: m.s.saidi@sharif.edu.
[*] Corresponding author2. Tel.: +61 (0)7373 53921; e-mail: trung.nguyen@griffith.edu.au

Highlights

- Cell spheroids are spherical aggregates best mimicking the tissue microenvironment.
- Spheroid culture better recapitulates the in-vivo condition in microfluidic chips.
- Microfluidics provides rapid spheroid formation with size uniformity and control.
- These chips contain microwells, microstructures, droplet generators, etc.
- To fabricate such chips, some design considerations must be taken into account.

Abstract

A cell spheroid is a *three-dimensional (3D)* aggregation of cells. Synthetic, *in-vitro* spheroids provide similar metabolism, proliferation, and species concentration gradients to those found *in-vivo*. For instance, cancer cell spheroids have been demonstrated to mimic *in-vivo* tumor microenvironments, and are thus suitable for *in-vitro* drug screening. The first part of this paper discusses the latest microfluidic designs for spheroid formation and culture, comparing their strategies and efficacy. The most recent microfluidic techniques for spheroid formation utilize emulsion, microwells, U-shaped microstructures, or digital microfluidics. The engineering aspects underpinning spheroid formation in these microfluidic devices are therefore considered. In the second part of this paper, design considerations for microfluidic spheroid formation chips and microfluidic spheroid culture chips (μSFCs and μSCCs) are evaluated with regard to key parameters affecting spheroid formation, including shear stress, spheroid diameter, culture medium delivery and flow rate. This review is intended to benefit the microfluidics community by contributing to improved design and engineering of microfluidic chips capable of forming and/or culturing three-dimensional cell spheroids.

Keywords: microfluidics, spheroids, tumor microenvironments; microwells; 3D cell cultures

1. Introduction

The term 'multicellular spheroid', hereafter abbreviated to 'spheroid', refers to *three-dimensional* (3D), well-rounded cell aggregations that consist of multiple single cells (epithelial, mesenchymal, endothelial, etc.). To form spheroids, cells suspended in culture medium are injected into specialized microenvironments in cell culture dishes or microfluidic chips, wherein they establish cell-cell interactions and form compacted, multicellular spheroid structures. A common misconception exists in the literature in relation to the term spheroid. Some loose aggregates or spatial distributions of cells in hydrogel droplets have been termed spheroid cultures, despite lacking cell-cell interactions. Hirschhaeuser *et al.* and Weiswald *et al.* emphasized that spheroids are compact and spherical in shape, not loose, easily fragmented cell aggregates [1, 2]. The compactness of spheroids endows them with several features analogous to those of *in-vivo* tumor tissues [3]. These features make spheroids a more suitable tool for *in-vitro* drug screening assays than two-dimensional (2D)-monolayer cell cultures [4].

In fact, several previous works have suggested that 2D-monolayer cell cultures should be replaced with multicellular tumor spheroids that better recapitulate the *in-vivo* environment [5-9]. Compared to 2D-monolayers, cancer cells cultured in 3D spheroids are more resistant to anticancer drugs [10-18] and photodynamic therapy [13], reflecting differences in cell secretions, hypoxia, species concentration, and proliferative gradients [8, 14, 19]. Furthermore, in 2D culture, cell-cell interactions are confined to the narrow common area between cells, while direct contact exists between each cell and both culture medium and the underlying culture substrate [15]. The substrate is usually made of polystyrene or other plastics which are impermeable and extremely rigid, unlike the natural tissue. At the same time, direct cell-culture medium contact in monolayer cultures leads to more significant exposure of cells to nutrients, oxygen, and drugs [20]. This often causes errors in estimating drug dosages required to kill cancer cells in actual patients. More broadly, several studies have illustrated that gene expression patterns are altered in 2D-monolayer cancer cell cultures, whereas results obtained from spheroids better recapitulate the molecular profiles of tumors *in-vivo* [21, 22].

An alternative approach for 3D pharmacological screening is the use of biopsied tumor tissues [19]. Although biopsied samples have historically been used for diagnostic purposes, they can also be employed as informative substrates for *ex-vivo* drug testing. However, it is challenging to access sufficient cellular material for such testing, mainly from metastatic sites. Furthermore, biopsied tissues experience both oxygen and nutrient depletion following surgical removal, as well as temperature variations and mechanical stresses that may adversely affect the tumor's microenvironment [23]. As such, 3D biopsied tumor samples lack necessary reproducibility [24] and compatibility with high-throughput drug screening approaches.

Compared to 2D cultures and biopsy samples, multicellular spheroids have several unique features that make them highly relevant models for *in-vitro* drug screening. First, 3D spheroids establish gradients in proliferation rate that result in creation of a cell layout consisting of three layers (Figure 1A): i) the proliferating layer - a rapidly proliferating layer comprising the outer 4-5 cell strata (60±10 µm thickness) [17] - which mimics sites adjacent to angiogenesis-induced capillaries; ii) the inactive *layer* - an inactive and inert intermediate layer, and; iii) the *necrotic core:* a hypoxic, necrotic core recapitulating tumor sites far from blood (which normally appear in large spheroids with diameters more than 500 µm [3, 17, 25, 26]. Second, 3D spheroids experience reduced drug, nutrient and gas exchange due to limited permeability. This generates steep, physiologically relevant gradients, particularly in large spheroids [1, 8, 27, 28] (Figure 1B). Third, cell-cell and cell-ECM attachments differ from 2D cultures to 3D spheroids, as well as between 3D spheroid cell layers. These interactions

strongly affect cytotoxicity assays. Fourth, spheroids have exponential growth rates [28, 29] that correspond to *in-vivo* data [30, 31].

Fifth, chemotaxis-driven cell movements – which exist in tumor tissue *in-vivo* [32, 33] – are also observed in spheroid cultures. Sixth, an acidic environment exists in the core of large spheroids (low pH) due to anaerobic activities and production of lactic acid [34] (Figure 1C).

Cell spheroids can also be formed from co-cultures (Figure 1D). These are advantageous for cancer research and regenerative medicine, as they better recapitulate the complexity of the natural tissue [35]. Such co-culture spheroids may be formed by cancer cells with fibroblasts [36], human umbilical vein endothelial cells [37], MC3T3-E1 cell [38] and pericytes [39]. Co-culture of hepatocytes and hepatic stellate cells (non-cancerous cells) was also performed in 3D spheroids by Lee *et al.* [40].

Although non-microfluidic methods [25, 28, 38, 41-55] for spheroid formation and culture have played essential roles in the development of this field, they are less efficient than microfluidic chips at mimicking *in-vivo* environments. Such non-microfluidic methods have deficiencies such as variable spheroid diameters, laborious handling, and low-throughput, which limit their efficacy in biological research. Moreover, the static microenvironment of a conventional microwell or hanging droplet (HD) culture plate causes the fast depletion of oxygen and nutrients while increasing waste concentrations and osmolality [56]. This directly influences spheroids and subsequent results from drug testing [57]. Other conventional methods such as spinner flasks and stirred-tanks [25, 53] are slow approaches that require large amounts of culture medium and space. These methods also result in significant variations in spheroid sizes, as well as harmful effects on cells, mainly due to shear stress [58].

Recent advances in microfluidics have contributed significantly to 3D spheroid research by addressing the aforementioned limitations [59, 60]. The significant advantages of microfluidic systems include providing controlled mixing [61], chemical concentration gradients, lower reagent consumption, continuous perfusion and precise control of pressure and shear stress on cells [62]. A remarkable feature of microfluidic chips is that cells can be cultured in a dynamic microenvironment to better recapitulate the tissue environment. Lee *et al.* reported that hepatocyte cell viability was lower in static cell cultures when compared with dynamic conditions in microfluidic devices after several days of culture [40]. Furthermore, Ruppen and co-workers experimentally demonstrated that cancer spheroids exposed to continuous perfusion of drugs showed higher resistivity than spheroids under static conditions (in a microwell plate) [8]. Indeed, continuous perfusion culture improves oxygen and nutrition supply for cells, as previously predicted computationally [63-67]. It has also been reported that gene expression profiles collected from hepatocyte cells cultured on a microfluidic chip with dynamic flow conditions showed more hepatocyte-specific characteristics than cells in static conditions [68].

There are several review articles in the literature about cancerous and non-cancerous spheroids, analyzing the conventional methods for spheroid formation [69-71], as well as the spheroid potential for high-throughput screening (HTS) [56, 72] and regenerative medicine [35]. Among the most recent of these, Hirschhaeuser and colleagues elaborated on the potential use of spheroids in cancer research as well as the importance of co-cultures and cancer stem cell spheroids [1]. In a comprehensive work, Nath *et al.* investigated conventional methods, novel non-microfluidic methods and on-chip microfluidic methods for spheroid formation, while also highlighting applications of tumor spheroids in cancer research [24]. Weiswald and co-workers discussed four spheroid models currently being used in cancer research, emphasizing their spherical shape and compact configuration [2]. Our group recently published a review on microfluidic methods for spheroid formation in which the biological applications of spheroids in organ-on-a-chip, body-on-a-chip, and organ-printing

were discussed [73]. However, we did not address the design considerations or cell trapping strategies for microfluidic systems from an engineering point of view. Other works have reviewed the importance of microfluidics in cancer cell culture and drug discovery [74-80], as well as considering various microfluidic chips enabling 3D cell culture with cancerous or non-cancerous cells [9, 81-86]. To the best of our knowledge, there is currently no review article available in the literature discussing detailed engineering features and design considerations for such microfluidic systems.

Herein, we refer to continuous-flow microfluidic chips that both form and culture spheroids in the same device as *microfluidic spheroid formation chips (µSFCs)*. Although there are numerous µSFCs, they can be divided into two principal categories: 1) those using emulsion-based techniques, or; 2) those utilizing microwells or U-shaped microstructures. Some other devices under investigation are culture-only chips, meaning that spheroid formation must first proceed using different methods outside the chip, before introduction to the chip for culture and drug efficacy testing [6, 8, 87]. We refer to these latter devices as *microfluidic spheroid culture chips (µSCCs)*.

This review discusses and categorizes various µSFCs and µSCCs based on their underlying spheroid formation mechanism and culture strategy, with a particular emphasis on engineering aspects. In the following sections, different continuous-flow µSFCs and µSCCs are first reviewed. Then, an introduction to various digital microfluidic methods for spheroid formation is presented. In the second part of this review, design parameters that enhance engineering of such systems are considered. Overall, this review collates design considerations and ideas from an immense body of published literature to support researchers in optimizing design and use of µSFCs and µSCCs.

2. Continuous-flow microfluidic spheroid formation and culture

Microfluidic platforms can be utilized for long-term perfusion cell culture while maintaining high cell viability, as shown in previous studies [6, 18, 39, 40, 88, 89]. Cell viability depends on the continuous supply of nutrients and oxygen, removal of waste products, low shear stress and the biocompatibility of materials. A number of characterization assays such as live/dead cell staining, drug testing, molecular profiling (e.g., FISH), as well as chemical, mechanical [90] and electrical stimulations are possible within microfluidic chips. These devices can also be coupled with on-chip tools for precise monitoring [91] and measurement of pH, oxygen level [92] and cell-secreted biomarkers [93], enabling a myriad of applications.

The µSFCs are designed to enhance the spheroid formation process by: providing size control; allowing rapid aggregation; requiring minimal interaction between the user and the device, and; replacing manual handling with engineered and automated procedures. These important capabilities have been achieved with the aid of transparent and biocompatible materials, in particular, poly (dimethylsiloxane) (PDMS) [94]. Given its hydrophobic nature and gas permeability, PDMS has been shown to be an ideal material for both spheroid formation and long-term perfusion culture with minimum cellular attachment [17, 94, 95]. Nonetheless, treatments with various chemical materials are frequently used to further enhance PDMS hydrophobicity. These materials include polyvinyl alcohol (PVA) [17], bovine serum albumin (BSA) [40, 88] and Synperonic F-108 [96]. Coating microchannel walls with a layer of poly (hydroxyethyl methacrylate) hydrogel has also been shown to optimize spheroid formation [13]. Contrastingly, as required for specific applications [94, 97], PDMS also can become hydrophilic by using plasma treatment.

2.1. Microfluidic spheroid formation chips (µSFCs)

The µSFCs can be categorized into two main groups that differ in spheroid formation procedure: emulsion-based spheroid formation and; microwell or U-shaped microstructure-based spheroid formation. Both have specific advantages and limitations that are briefly discussed in the following sections. First, the emulsion-based techniques are considered to

evaluate the most critical parameters involved. Second, microwell and U-shaped microstructures are discussed along with their working principles and challenges. Moreover, the hydraulic-electric analogy for proper design of μSFCs is introduced.

2.1.1. Emulsion-based techniques

Flow-focusing droplet generators have been the subjects of many studies due to the uniformity in droplet and spheroid sizes produced by them, as well as their high-throughput continuous operation [98]. Single- (Figure 2A) [36, 99, 100], double- (Figure 2B) [101, 102] and triple- (Figure 2C) [98] emulsion droplet generation techniques have been utilized in μSFCs. Flow focusing devices for this application exist in either axisymmetric [101] or non-axisymmetric [36, 98, 103] configurations. The nature of this method facilitates the fast production of microdroplets and thus high-throughput spheroid formation (HTSF). Droplet generation frequencies up to 50 droplets per second [104] and 200 droplets per minute have been achieved using collagen [99] and alginate [105] hydrogels.

Several liquids are used for cell encapsulation and spheroid formation in μSFCs with different configurations around the core flow. Cell suspension (CS) in oil (O) emulsion (i.e., CS/O) [106] and cell-dispensed hydrogel (Gel) in oil (i.e., Gel/O) droplet generation [36, 107] are among the single-emulsion methods which are widely used. Cell suspension in oil in culture medium (CM) (i.e. CS/O/CM) [102] and CS/Gel/CM [101] are double-emulsion techniques. The CS/Gel/CM double-emulsion technique can enhance droplet uniformity and entrap cells firmly within the droplet. It is facilitated by encapsulating the cell-containing core droplet within an alginate hydrogel shell [101, 108] that acts as an impermeable barrier with respect to the cells. However, in contrast to the CS/O/CM method, gelation is required in the CS/Gel/CM method. Using mineral oil as a barrier instead of hydrogel enhances oxygen transport to the droplets, reflecting the higher permeability of mineral oil to small molecules [109]. Although these barriers produce nutrient concentration gradients within the droplets, they act as an interface between the culture medium and the encapsulated cells which protects cells from high shear stress.

Hydrogels in emulsion spheroid formation

High proliferative cancer cells quickly aggregate with a spheroid shape after being encapsulated in a hydrogel droplet [98]. However, other cell types such as mesenchymal stem cells are not able to form spheroid aggregates in a solid-like hydrogel [58]. The high concentration of alginate and agarose [110] causes higher stiffness and disturbs cell proliferation [108]. Yu *et al.* reported that alginate concentrations around 3% (v/v) and higher reduce the proliferation of encapsulated tumor cells within droplets due to high rigidity [108]. They found that alginate concentrations of 1.5% (v/v) to 2% (v/v) are suitable for spheroid generation, permitting cell proliferation while still entrapping cells firmly within droplets - despite low alginate concentrations.

The solid core formed after droplet gelation not only hinders cell proliferation but also prevents cells from establishing the cell-cell interactions necessary for compact spheroid formation. However, this problem is resolved by the aid of matrigel. As matrigel is digestible by cells, the solid core is degraded after a short time and the adverse effects disappear [107, 111]. As a result, mixtures of alginate and Matrigel (1:1 v/v) for cell-dispensed core flow generate droplets with enhanced droplet uniformity as well as yielding spheroid formation in a shorter time [107, 112].

Collagen, a typical hydrogel existing in our body, has priority over other hydrogels for cell culture as it can properly mimic the *in-vivo* microenvironment. In conventional methods, collagen droplets are made via emulsification [113] or simple droplet dispensing [114-116]. As a consequence, the resulting droplets have non-uniform diameters due to the coalescence of microdroplets before gelation. Cell viability assays also indicate that centrifugation-aided

collagen droplet formation causes cell death in droplets as a consequence of centrifugal and compressive forces exerted during the microsphere extraction process [99].

Microcapsules having liquefied alginate in the core, in addition to poly (L-lysine) and alginate as barriers, are also utilized for spheroid formation. In these methods, the alginate bead that fills the core is liquefied with tri-sodium citrate treatment [117], despite such treatment being reported to perturb live encapsulated cells [98]. Another drawback is the excess pressure and mechanical stress imposed on spheroid cells by the alginate-poly (L-lysine) barrier, which adversely affects cell proliferation and final spheroid size [98, 101]. Sodium citrate is also used for liquefying alginate microdroplets after gelation to facilitate the retrieval of spheroids formed within the droplets [100].

Droplet stabilization

Chan *et al.* reported that the use of amphiphilic surfactants (i.e., showing both hydrophobic and hydrophilic behaviors) helps to maintain droplet stability [102]. They also reported an acceleration in spheroid formation by decreasing the duration time from one day to 150 minutes. Moreover, they monitored spheroid formation using labels for collagen type I and laminin, as well as immunostaining for E-cadherin and integrin-α5β1 to assess cell-cell and cell-matrix interactions and adhesions. Kim *et al.* used glycerol to adjust viscosity in the cell suspension constituting the core flow in an on-chip CS/Gel/CM spheroid generation method [98]. Given that viscosity was increased, the cross-sectional geometry of the droplet took a more circular form. However, glycerol had devastating effects on cell viability, reducing it to just 13% in a glycerol concentration of 20% [98]. Using viscous oil as the droplet shell instead of a hydrogel obviates the need for viscosity adjustments in CS/O/CM method [102]. Adding Span 80 surfactant to the mineral oil further stabilizes the droplets formed in the CS/O single-emulsion technique [99, 105, 107].

Flow rate

In emulsion-based techniques, droplet generation frequency and droplet diameter are adjustable by varying the flow rates. Smaller droplets are normally obtained by increasing the rate of sheath flow [102]. In addition, the thickness of the capsule shell can be adjusted by changing the flow rates of different phases [101] or varying the channel dimensions of the microfluidic device [102]. In fact, the shell thickness is related to the ratio between the volume flow rates of the sheath and core flows [98]. Flow rate is also crucial for droplet anchorage after droplet generation [36, 103]. The flow should be adjusted to allow the droplets to settle in traps designed for spheroid formation and culture. High flow rates push the droplets towards the outlet; whereas, low flow rates cause channel clogging in some μSFCs [36, 104].

Droplet anchorage and retrieval

Proper droplet anchorage is crucial for on-chip gelation, culture perfusion, spheroid formation and drug screening. Multiwell plates [100, 105], Petri dishes [107] and cell culture flasks [108] have frequently been used for droplet storage. However, these platforms do not inhibit droplet coalescence. Several microfluidic chips have been designed which can facilitate high-throughput droplet anchorage with hundreds of anchoring sites, solving this problem. One configuration contains a vast number of droplet arrays. Each array has tens of anchor sites which resemble two out-of-phase sinusoid functions placed in parallel (Figure 3A) [36, 103].

Droplets squeeze through the narrow passing throats one by one to reach the downstream trap, driven by pressure exerted on them via pumping. The design principles in this configuration are based on droplet size, viscosity and surface tension, which together shape device performance. The flow rate and the resulting pressure gradient along the channel also play essential roles in avoiding droplet coalescence. Although droplet coalescence has been prevented by this method, both throat and trap sizes must be designed to properly facilitate droplet squeezing and anchorage without droplet differentiation

.

McMillan *et al.* fabricated a µSFC having a high-throughput droplet storage array consisting of 2000 droplet sites that suited radiation assays performed on tumor spheroids (Figure 3B) [103]. However, it was not possible to have a culture medium or drug solution flow through the microchip since the design had been set for radiation assays. Sabhachandani *et al.* generated a similar design that was able to facilitate a continuous flow of medium and drug [36]. The only possible problem remaining with this anchorage design is flow blockage. As the medium flows continuously, the induced pressure gradient pushes droplets downstream, such that a gelled droplet may be pushed to the outlet of its trap, thereby blocking the flow. The presence of a gap between traps and the bottom surface of the top PDMS layer can eliminate this problem by permitting continued medium flow. In another design by Tomasi *et al.*, the chip contained over 5000 microwells for droplet storage [104]. They used V-shaped trails to distribute generated droplets homogeneously over the anchoring microwells (Figure 3C). The strengths of this device include rapid droplet generation, with 10-50 droplets formed per second - filling all 5000 available anchors in less than 10 minutes.

Immediately after droplet formation, the surrounding sheath fluid usually has to be removed and replaced with culture medium or drug solution. In one design this was achieved through the application of magnetic forces using magnetic nanoparticles [105] immediately after on-chip droplet formation. Nanoparticles were dispensed into the cell suspension to cause a deviation in the droplets' path within the magnetic field. Consequently, droplets leave the oil stream and enter the culture medium, enabling their retrieval (Figure 3D). Wang *et al.* guided microdroplets in oil to a microwell on the chip which contained culture medium in its lower half (Figure 2A) [100]. Thus, after sedimentation, droplets were easily extracted from the culture medium for further use.

2.1.2. Microwells and U-shaped microstructures

In the last decade, a large number of microfluidic platforms have been designed for spheroid formation and culture using microwells [6, 7, 39, 96] or U-shaped microstructures [16, 18, 118-121] embedded in the device. These structures are designed to help spheroid generation within a shorter period [122, 123], with controllable and uniform diameters [124, 125] and a compact spheroid shape [17, 120]. Recently, we employed numerical simulations to find the necrotic core and hypoxic zone in a U-shape system containing spheroid [126] and compare the performance of such system in microfluidic platforms with either U-shaped barrier or microwell structure containing cell aggregates in toroidal shape [127].

U-shaped microstructures function either temporarily, using pneumatic actuation (Figure 4A) [119-121, 128], or permanently within the device (Figure 4B-C) [118, 121]. Liu et al. fabricated µSFCs which had temporary U-shaped pneumatic microstructures for high-throughput spheroid formation, culture assessments and drug efficacy tests (Figure 4A) [120, 128]. A large number of these U-shaped microstructures are usually embedded (e.g. 360 [120], 28 [18], 512 [129]) in each chamber of µSFCs to trap most of the cells introduced into the chip [18, 118, 120, 121, 128]. Spheroid diameters depend on microstructure size, while the relative position of microstructures is essential for efficient cell trapping. Kim *et al.* investigated cell trapping efficiency and related design optimization using computational fluid dynamics (CFD) simulation first, followed by experimental validation [130]. The detailed information regarding CFD simulations of U-shaped microstructures can be found in the recent work of Zhang *et al.* [129].

Hydrogel droplets can also be trapped within these microstructures [18]. Yu *et al.* designed a µSFC, named *microsieve*, containing triple-portion U-shaped microstructures to trap cell-containing alginate droplets (Figure 4B) [18]. Since cells were trapped within a hydrogel droplet, diffusion of oxygen and other species to the cells from culture medium was limited. Therefore, the design was enhanced by introducing junctions between three microstructure portions, thus facilitating better oxygen and nutrient transport.

The fluid flowing towards a microstructure creates a stagnation region in its front. Consequently, species transport is facilitated via diffusion rather than a convective mechanism [121]. This stagnation region exerts forces on cells residing in the microstructure, thereby inducing more cell-cell interactions and faster spheroid formation [121]. Hence, spheroid formation time can be adjusted by flow rate, since the formation is affected by the stagnation pressure existing in front of the microstructure. However, high flow rates cause cells to escape from the narrow space between the microstructure edge and the PDMS slab [120, 121]. On the other hand, to hold spheroids within microstructures the flow should be sustained, thereby maintaining the necessary stagnation pressure [121]. Otherwise, the spheroids exit U-shaped microstructures and flow towards the outlet (Figure 4C).

Microwell-based µSFCs have been utilized more than other techniques due to their simplicity and ease of operation [131-133]. In general, a microwell-based µSFC needs a specified number of microwells and a microchannel network to deliver the culture medium (Figure 5A-E). For spheroid generation, the cell suspension is introduced at the inlet, usually with a cell density of 105 to 107 cells/ml [6, 68, 96], depending on the cell type (Figure 5A). To achieve uniform cell seeding in microwells and uniformly sized spheroids, the cell suspension should fill the device entirely before cells begin to deposit in the microwells. The cells take several minutes to deposit on microwell bottoms and channel floors (Figure 5B). Excess cells that did not enter microwells should be rinsed out of the chip to avoid subsequent channel clogging [7, 68, 134] (Figure 5C). After that, cells begin to adhere to each other, form a spheroid (Figure 5D), and continue their growth with a continuous or intermittent supply of fresh culture medium (Figure 5E). Using more than one inlet and microwell-contained channel allows testing drugs with various concentrations, cell types and different spheroid sizes on a single microfluidic chip [134].

Microchannels should be designed in a way that can prevent undesirable spheroid escape from the microwells (Figure 6A-F). Choi *et al.* [68] reported cells and spheroids escaping from the microwells when high flow rates were utilized in the main channel. Experimentally, it has been indicated that increasing the channel width [134] or decreasing its height [17] can limit spheroid escape. However, sometimes it is required to retrieve spheroids for flow cytometry analysis, stem cell differentiation-assays, etc., which necessitates spheroid ejection from the microwells. Rousset and colleagues performed a CFD study to obtain the flow rates necessary to deliver a sufficient lift force on spheroids to drive their exit from microwells [65]. However, these flow rates might create high shear stress on cells while pushing them upward. Therefore, an acceptable shear stress threshold (1 Pa) was applied as a constraint when calculating optimum geometrical parameters based on numerous simulations [65].

In order to equalize flow rates across several microchannels, flow resistance must be the same through all of them. Therefore, if channels have the same width and height, their lengths must also be equal to satisfy this requirement. Sinuous channels, often used in concentration gradient generators (CGGs) as mixing channels, are appropriate to adjust channel length

precisely within a small area of the chip. Such channels can thus be applied for flow control purposes rather than including valves within microfluidic chips [88, 135].

Desired flow rates must also take into account the number of cells existing in the culture environment and their corresponding requirements for oxygen, nutrients and other factors. This is complicated by the fact that various species have limited solubility in water at any given temperature. For instance, this value is 1 gr/cm^3 [136] for glucose and 0.007 gr/cm^3 for oxygen in water at 37 C$^\circ$ [137]. Hence, one should consider both the amounts of these species present in culture medium and the corresponding uptake rates achieved by cells. However, these calculations are not sufficient to ensure that hypoxia or anoxia are avoided in the center of a spheroid cultured on a chip. The limited diffusion of glucose and oxygen to spheroids, combined with the specified geometry in which the spheroid is cultured, make the problem unpredictable. Thus, mathematical and numerical analyses combined with experimental investigations are needed [64-66, 138-140].

A major drawback of microstructure- or microwell-based µSFCs is their limited application for HTS. In other words, simultaneous drug tests with various combinations and concentrations have rarely been carried out on a single µSFC due to the lack of a suitable microchannel network. Most µSFCs, while achieving HTSF capacity, permit only one concentration of a drug, or one combination of drugs, to be applied to spheroids at any given time. Therefore, one has to employ several chips for each single drug concentration. Recently, Kwapiszewska *et al.* [6] and Zuchowska *et al.* [141] designed microwell-based µSFCs that facilitate simultaneous exposure of spheroids to different concentrations of the 5-fluorouracil anticancer drug. This advancement was achieved by coupling the µSFC with a CGG. In this design, microwells were arranged in a configuration compatible with commercial microplate readers for automated monitoring (Figure 6D).

Hydraulic-electric analogy

The hydraulic-electric analogy has helped microfluidic engineering integrate microfluidic chips with pressure drop adjustments and precise flow rates [142]. In designing µSFCs [16, 39, 88] and µSCCs [8], the hydraulic-electric analogy has been used to direct the path of suspended cells or spheroids to desired on-chip locations (i.e., microwells, cell traps, etc.). By using this method, channel width, height, and length are computed to achieve desired flow rates and pressure drops. As the flow velocity and length scales are very small in microfluidic chips, the Reynolds number is usually below unity [143], thus ensuring a laminar flow regime [144, 145]. This fact helps designers efficiently compute flow rates, resistances and pressure drops by using the Poiseuille pressure drop equation in microchannel networks [146, 147]. In the hydraulic-electric analogy, the electric potential difference is analogous to the pressure drop, electric current corresponds to flow rate, and electrical resistance plays the role of the flow resistance [142]. This analogy introduces an acceptable method for flow calculations in biological microfluidics [8, 11, 16, 88, 135, 148].

One design used two sets of channels named trapping and bypass. The channels had different resistances in order to divide flow rates such that the larger part of the fluid passed through the trapping channel while a small amount of fluid entered the bypass channel. Spheroids reaching the split in the channel are forced by the upstream flow to enter the trapping channel, thereafter stopping in the trap neck and blocking the flow inside that channel. This prevents further spheroids from entering, such that these move into the bypass channel and get trapped in the next empty trapping channel [8, 11]. McMillan *et al.* [149] designed a nearly identical device to trap cell-containing alginate droplets instead of spheroids. This mechanism has recently been adapted for single cell trapping by modifying the geometry and fluidic parameters [150].

In other works by Kim *et al.* [88, 135] and Ruppen *et al.* [39], the spheroid formation was achieved by driving a cell suspension towards individual microwells for sedimentation trapping (Figure 6E and F). In this design, each microwell is supplied by a dedicated

microchannel. This contrasts with typical microwell-based µSFCs, wherein one microchannel usually feeds tens of microwells [68, 134]. Nonetheless, flow rates and geometries must still be optimized such that cells can sediment without easily escaping through the exiting channel. For instance, if the channel height equals the entering one, most cells pass through the microwell and are lost. Therefore, the exiting channel has a reduced height relative to the entering one, enhancing trapping. Kim *et al.* [88, 135] used 190 µm and 25 µm while Lee *et al.* [16] utilized 300 µm and 5 µm for the entering and exiting channel heights, respectively.

Cells start to sediment as soon as they enter the chip, with the sedimentation rate depending on cell diameter as well as fluid properties such as kinetic viscosity and density. To promote successful cell trapping, it is required that cells roll on the channel floor when arriving at the microwells [135] making the average flow velocity a significant parameter. Kim *et al.* [135] performed a numerical simulation for modeling this phenomenon by considering the cells to be 10 µm in diameter and taking cell-wall and cell-cell interactions into account. According to the flow rates and channel dimensions reported by Kim *et al.* [88, 135], the suitable average flow velocity can be calculated to be approximately 300 µm/sec [88] and 500 µm/sec [135] in the channels. With these velocities, no shear stress-induced cell damage was declared; meanwhile, cell trapping was carried out successfully [88, 135].

Lee *et al.* designed a hydrostatically-driven flow µSFC based on the hydraulic-electric analogy [16]. After introducing the cell suspension at the inlet, the device was tilted by 90 degrees to promote cell sedimentation into the trap chambers for spheroid formation. The authors adjusted the height of the exiting channel of the trap chamber such that its flow resistance was approximately one thousand times larger than that of the main channel. Therefore, the flows conducted through the trap chambers were identical. After spheroid formation, the spheroids could be perfused under continuous culture medium flow or retrieved by changing the flow direction in the device (Figure 16D) [16].

2.1.3. Other microfluidic chips for spheroid formation

In this section, we describe other microfluidic designs for spheroid formation and culture including pyramid microwells, porous membranes, and microrotational flow. Their pros and cons are discussed briefly to help designers create their microfluidic chip more efficiently.

Torisawa *et al.* designed a µSFC containing pyramid-shaped microwells with holes at their vertex to facilitate on-chip scanning electrochemical microscopy (SECM) (Figure 7A) [151]. The spheroid formation took place in the microwells first. Afterwards, the microwells were inverted to perform SECM analysis while spheroids were hanging from the microwells, a configuration resembling the HD method.

Porous membranes have been used in µSFCs to dictate cell patterning necessary for on-chip mono- [155] and co-cultured [156] spheroid formation. Figure 7B shows a two-layered hydrostatically-driven µSFC in which a porous membrane was placed between the two layers to filter cells behind its pores. Each layer of the µSFC had microchannels, some of which were connected to microchannels within the other layer using the porous membrane [156, 157]. Hsiao *et al.* placed the spheroid formation chambers lateral to the main channel of the top layer, facilitating single spheroid formation and enhancing size uniformity [156]. Kuo *et al.* used the same principle for spheroid formation with pores being 10 µm in diameter while in other similar devices, the pore size was 5 µm [155]. The cell trapping efficiency of the device was at most 97% which signified its low cell waste. Recently, we have shown that 3D spheroid culture is possible on electrospun PDMS nanofibers [158]. By integrating this membrane in a microfluidic platform, several biological studies on 3D cell culture samples would be feasible.

Microrotational flow was proven to induce spheroid formation in microfluidic chips by Ota *et al.* [122, 123, 152] (Figure 7C). This method mediated spheroid formation with

acceptable size controllability and short times - as rapidly as 120 seconds. Spheroid sizes ranging from 130 to 430 µm with a standard deviation of less than 17.2% can be achieved by changing cell concentration in the cell suspension entering the device. In the first design, spheroids could be cultured only for one day because the spheroids started to exit from the chambers afterwards [123]. In the second design, the device was integrated to facilitate HTSF [122]. Even though spheroids remained in the chambers for more than one day, unwanted cell aggregates still existed and had to be removed by a filter. This indicates that a fraction of cells introduced to the device did not take part in the spheroid formation process and were therefore wasted. Another deficiency of this method is that it requires a large volume flow rate of culture medium (1.2 ml/min) in comparison with microwell-based techniques [122, 152].

Sound waves were recently used by Chen *et al.* [10] in a novel µSFC that integrated 3D acoustic tweezers (Figure 7D). The device could simultaneously form 150 spheroids within less than 30 minutes using various cell lines including HepG2, HEK 293, SH-FY5Y and HeLa cells. The rapidity of spheroid formation limited the necessary exposure time of cells within the acoustic field, reducing cell death caused by sound waves.

A microfluidic design exists that provides steady-state perfusion to spheroids [159] or cell aggregates [153, 160] while avoiding shear stress on the cells. In this design, micropillars were used to minimize the direct exposure of spheroids to the flow of culture medium, confining the transport phenomena to diffusion - as occurs in *in-vivo* microenvironments. To culture spheroids in this chip, pre-formed spheroids were inserted into the center channel and then the flow of culture medium was established through the side channels [159] (Figure 7E).

Tung et al. [54] designed a novel HD platform (Figure 7F) to optimize the procedure traditionally used for HD spheroid formation [161]. The platform was compatible with liquid handling robots as well as conventional 384 & 96-well plate readers utilized in high-throughput drug screening. Although these advancements were significant for the spheroid formation and culture experiments, inherent design characteristics limit the capacity to properly mimic *in-vivo* microenvironments. Liquid evaporation within the wells and droplets leads to increased osmolality that can negatively impact cell viability [54, 162]. Specific amounts of culture medium should be interchanged manually with the delicate droplets every day to compensate for the evaporated liquid.

Recently, the inability to establish dynamic microenvironments in HD platforms has been solved by novel HD-based microfluidic designs [154, 163]. In a valuable work by Yazdi *et al.* [154], both pulsatile and steady-state flows were created through the device by pneumatic actuation, mimicking the *in-vivo* microenvironment and thereby enhancing the culturing of human cardiac iPS-derived spheroids (Figure 7G). These platforms enabled closed-loop circulation of medium, but still required the addition of fresh culture medium to compensate for evaporation [163].

2.2. Microfluidic spheroid culture-only chips (µSCCs)

µSCCs are designed to provide suitable microenvironments for cell spheroid culturing and drug tests. Importantly, cell spheroids must first be formed using other platforms and then transferred to a µSCC. Perhaps reflecting this limitation, µSCCs are not as prevalent as the µSFCs in the literature. Indeed, spheroid retrieval and transfer, combined with spheroid formation using other devices (conventional techniques), may make this approach relatively laborious and expensive in terms of time and experimental cost. Nonetheless, in this section several µSCCs are described for a better understanding of these devices.

Munaz *et al.* fabricated a µSCC which had a wide main channel followed by parallel narrow microchannels of 80 µm width, 60 µm apart from each other [87]. Pre-formed spheroids were injected into the chip through the main channel and hydrodynamically directed to the narrow microchannels. The spheroids were trapped behind the narrow microchannels at a flow rate of 30 µl/min. The authors reported that flow rates above 60 µl/min led to spheroid disaggregation due to high shear rates (Figure 8A). Ruppen and

colleagues also designed a µSCC using the hydraulic-electric analogy so that flow resistance in bypass channels was more than trapping channels, facilitating efficient spheroid trapping (Figure 8B) [8]. They reported that shear stress was negligible and did not affect the cells since there were negligible flow rates through the trapping channels where spheroids were trapped.

Kim *et al*. designed a µSCC that had eight microchambers for spheroid culturing [89]. Following loading, the spheroid entered a microchamber which resembled a vertical hollow cylinder. In the device, culture medium flow was generated by tilting the platform (Figure 8C). Astolfi and co-workers designed a microfluidic chip to culture micro dissected tissues whose sizes were identical to cell spheroids (380 µm in diameter) [139]. Their design included a channel that contained several flat-bottomed microwells to trap the dissected tissues (Figure 8D). Using simulation, they determined that high flow velocities caused these tissues to escape from the microwells, while the simultaneous shear stress was not high enough to have adverse effects on cells.

Some multi-organ-on-a-chip devices use liver spheroids as the suitable 3D culture for liver lobules [164, 165]. In fact, the spheroids are introduced to the specific chambers and microchannels on the chip to be co-cultured with other organs such as pancreatic microtissues [165], skin tissue, intestine, and kidney cells [164]. The circulatory flow within the device exposes the spheroids to the metabolites and the materials secreted by other organ cells to mimic the in-vivo relations and functions of the organs.

3. Digital microfluidics in spheroid formation and culture

Digital microfluidics is a state-of-the-art technique used to handle picoliter to microliter liquid droplets [166, 167] using different mechanisms such as the Marangoni effect [168], magnetic fields [169, 170], optical actuation [171] or electrostatic forces [172-174]. Recently, much attention has been given to the application of this format of microfluidics in various biomedical applications including assisted reproductive technology and in vitro fertilization [175]. It has been shown that the electrostatic fields used in digital microfluidic chips have negligible effects on cell viability, morphology [174, 176] and gene expression [172], making such platforms suitable for both 2D [174, 176, 177] and 3D [172, 173, 178] cell culture. This microfluidic approach has facilitated more realistic and accurate experiments than those carried out in multiwell plates for toxicity screening [172, 179], invasion assays [173] or cell polarization assays using spheroids [172]. In this method, liquid droplets are introduced into the chip to form sub-droplets (passive dispensing) and directed to HD holes (Figure 9A) [180] or hydrophilic sites (Figure 9B) [181, 182] to be anchored. The sub-droplets take the shape of HD holes or hydrophilic patterns and are therefore outstanding at creating the desired droplet structures [178]. It is also possible to deliver reagents, drugs and any other liquid solutions to the anchored droplets on the chip without any pumps or valves [178].

Using on-chip crosslinking, Eydelnant and co-workers created cell-containing microgel structures in a digital microfluidic chip [178]. They reported spheroid formation from Madin Darby canine kidney (MDCK) cells in Geltrex and type I collagen microgel structures. They successfully probed on-chip spheroid polarization and 3D kidney epithelialization. Another digital microfluidic chip was designed for hepatotoxicity and albumin analysis as well as enzymatic activity assays on liver HepG2 spheroids [172]. The device performed droplet merging, mixing and splitting as well as dilution of solutions by digitally actuating the droplets on the chip. Another platform used HDs on the chip to form fibroblast and colon cancer cell spheroids for invasion assays [172]. Although digital microfluidics appears to have numerous advantageous, it nonetheless suffers from some deficiencies including liquid

evaporation, lack of continuous perfusion, complex control and fabrication [167] as well as biofouling [179]. Some of these limitations have recently been addressed, but others remain to be eliminated.

4. Statistical comparison and a brief summary of µSFCs and µSCCs

Figure 10 compares the standard deviation (SD) of spheroid diameter and formation time duration resulted from various spheroid formation methods. The formation time is considered as the time elapsed before cells make an aggregate in the culture as reported by the authors. As seen in the figure, the emulsion and the liquid overlay technique have the smallest and the largest SDs. Microrotational flow device had the shortest formation time due to the specific flow field in this condition which brings the cells close to each other, sufficient for developing cell-cell bonds in only 120 seconds. The well-based methods, although having larger SDs, facilitate spheroid formation in a shorter time than the emulsion technique. Occupying the smallest SD and formation time amongst the conventional methods, the HD method appears to be the best one which is comparable with the microfluidic methods.

There are more than 40 cell types used on various µSFCs and µSCCs so far, which are mostly the cell lines presented in Figure 11. Primary cells such as lung adenocarcinoma [39] and rat hepatocyte cells [68] have been rarely used in single- [68] and co-culture [39, 89] with other cell lines on µSFCs [39] and µSCCs [89]. The majority of µSFCs and µSCCs conducted chemosensitivity tests using anticancer drugs such as duxorubicin [134], paclitaxel [134], cisplatin [7], 5-fluorouracil [10] while only two works recently presented photodynamic therapy on lung (A549 and MRC-5) [183] and breast cancer cell lines (T47D, MCF-7 and SUM159) [13] on µSFCs.

For summarizing the information presented in Section 2, a table is added briefly show the microfluidic spheroid formation and culture types along with their advantages and disadvantages.

5. Design considerations and affecting parameters of µSFCs and µSCCs

Several parameters influence the microfluidic environment of a spheroid cell culture as illustrated in Figure 12. The impacts and traits of these parameters should, therefore, be investigated properly prior to design and fabrication. In this section, some of these key parameters are discussed to provide helpful guidelines for efficient µSFC or µSCC development.

5.1. Microstructure design for spheroid formation and culture

Hemispherical or U-shaped microstructures are appropriate geometries for guiding uniformly sized spheroid formation. When a number of cells are trapped within a hemispherical geometry, the resultant microforce exerted on the cells by the round wall improves spheroid compaction since the force focuses on the center (Figure 13A). Therefore, the bottoms of microwells and cell trapping microstructures in multiwell culture plates and µSFCs are designed as concave shapes [6, 39, 40]. This hemispherical shape also helps with the single spheroid formation in each microwell [39, 184]. Ruppen *et al.* suggested that after two days of culture, most of the concave-bottomed microwells contained one spheroid, while flat-bottom microwells mostly contained two or three [39].

One method to create concave-bottomed microwells in PDMS microfluidic chips is to fabricate flat-bottomed microwells first and then pour PDMS prepolymer on the microwells. Next, the prepolymer should be raked out by a flat plate (Figure 13B). The remaining prepolymer in the flat-bottomed microwells forms a concave geometry due to surface tension between the PDMS liquid prepolymer and the PDMS solid surface [40]. Xu and colleagues proposed a novel method for concave-bottom fabrication by controlling the temperature and pressure of trapped air bubbles [125]. They fabricated the desired number of microcavities on a poly (methyl methacrylate) plate. PDMS was poured onto the plate but it did not fill the microcavities due to its high viscosity. To achieve this viscosity, the PDMS was cooled to -20˚C. By increasing the temperature and reducing the pressure in an incubator, the air bubbles expanded and pushed up the adjacent PDMS layer to form the desired concave microwells (Figure 13C). Ruppen *et al.* used a fabrication procedure, involving four different castings, to make concave-bottomed microwells [39]. First, flat-bottomed microwells were fabricated using stereolithography (3D printing). Following double casting with silanization, the flat-bottomed microwells were transferred to PDMS. Then, uncured PDMS droplets were deposited onto micropillars to form the desired hemispherical shapes. Last, the final mold was obtained by casting an epoxy onto the PDMS hemispherical substrate (Figure 13D).

Pneumatics can also be used to generate temporary microwells or U-shaped microstructures in µSFCs. Anada and co-workers generated membrane deformations by establishing pressure differences across a thin, flexible PDMS slab, thereby producing concave-bottomed microwells [185]. After spheroids were formed, the pressure difference was eliminated. As a result, the microwells completely disappeared and the spheroids were delivered at the outlet.

Permanent [118, 121] and temporary pneumatically-actuated [119, 120, 128] U-shaped microstructures were fabricated on PDMS µSFCs inside microchannels. Unlike temporary U-shaped microstructures, the permanent ones were inflexible and consequently did not allow proper spheroid retrieval. Poly (ethylene glycol) diacrylate, which is a non-adherent hydrogel, was also used instead of PDMS to fabricate the U-shaped microstructures [118].

The design of spheroid culture microenvironments in µSCCs usually have the intended characteristics to facilitate the specific test on the spheroids. In a recent design, the authors investigated the effect of shear stress on chemoresistance and stemness of ovarian cancer spheroids in a µSCC [186]. The chip consisted of 4 mm wide and 250 µm height

microchannels suitable for exposing the spheroids under controlled shear stresses of 0.02 and 0.002 dyne/cm^2. In a design by our group, spheroids were introduced to a µSCC for fusion of olfactory ensheathing cell spheroids [87]. The device contained parallel narrow channels after a wide chamber behind which spheroids trapped. The channels were close enough to enable the spheroids make bonds between themselves while being under culture medium perfusion. For drug toxicity, various designs exists which differ in the mechanism of spheroid trapping and culture [8, 89, 139]. They share a mutual feature which is having spheroid culture sites far from direct exposure of spheroids from the flow of culture medium. The primary goal of the design in these devices is to avoid the spheroids from high shear stresses to remove any chances of cell death caused by it.

5.2. Culture medium delivery

The µSFCs and µSCCs are designed for various purposes such as drug cytotoxicity assesment [39], study the effect of shear stress on the spheroids [186], multi-organ culturing [164] and various other applications not developed yet. With this in mind, various flow conditions in the chip are needed that the designers should be familiar with them. A number of pumping methods are currently used within microfluidic chips for delviery of the culture medium [187]. These include: hydrostatic pressure differences [16], peristaltic micropumps [123, 188], osmotic pressure differences [40, 68, 189], passive pumping [190] and syringe pumps [88, 98].

In hydrostatic pumping, the pressure difference comes from the difference between the liquid levels of the inlet and outlet ports (Figure 14A). To maintain a fixed flow rate in microchannels, one needs to add liquid to the inlet or remove it from the outlet reservoirs which otherwise the flow rate becomes transient [7, 89, 155]. In HD-based µSFCs where culture medium experiences high rates of evaporation and osmolality changes, the transient flow cannot perfectly control the medium solute concentrations. Recently, Ong *et al.* designed a hydrostatically-driven µSFC in which the flow rate maintained constant to address the problem of transient flow [191].

Peristaltic pumping is used within cell culturing microfluidic chips [187]. Mousavi *et al.* designed a thermoplastic polyurethane diaphragm adopted from a plug-and-play microvalve to facilitate peristaltic fluid pumping for cell culture applications (Figure 14B) [188]. Peristaltic pumping is widely used for imposing cyclic shear stresses on endothelial cells [187] and also to better mimic the *in-vivo* blood flow for cardiac microtissue spheroids [154].

Osmotic pumping has been used in µSFCs for continueous medium supply to hepatocyte spheroids [40, 68]. In osmotic pumping, adjusting the concentration of the driving agent (such as polyethylene glycol) enables flow controllability [40, 68]. Fabrication is possible by simply gluing a cellulose membrane as a window to a PDMS chamber containing water [192] (Figure 14C). Although it enables nanoliter flows, the flow rate decreases as the time goes by due to the gradual reduction of the driving agent and requires constant refilling of the medium chamber and driving agent.

In µSFCs and µSCCs this type of flow condition provides time-variable supply of nutrients while the cell spheroids consume the nutrients and produce metabolic wastes constantly.

Passive pumping is also a practical method for microfluidic cell culture. As reported by Berthier and Beebe [190], the flow has two phases in this system. In the first phase, the flow is almost constant which is the most noticeable feature of this method. However, in the second phase, the flow velocity decreases in the microchannels until it ceases. It is possible to refill the inlet droplet manually to maintain the flow; however, it would be laborious to maintain such perfusion for long-term culture (Figure 14D).

Among the above-mentioned techniques, despite being costly and occupying a large space, syringe pumps are often the most practical and suitable pumping method. They operate automatically and are programmable, enabling steady state, continuous flow throughout the

chip which is needed in most experiments in which tumor spheroids are under chemosensitivity studies [39, 149, 193].

5.3. Shear stress

One of the most crucial considerations in microwell and microchannel design within µSFCs and µSCCs is the shear stress to which cultured spheroids are exposed, since high shear stresses may cause spheroid disaggregation [40]. More subtly, Chang *et al.* reports that high shear stress on cancer cells modifies cell cycle, differentiation, and gene expression profile [195]. The maximum allowable shear stress on various mammalian cells, reported by different authors, falls into a large range from 0.001 [196] to 10 dyne/cm^2 [197]. This illustrates that acceptable shear stress differs for distinct cell lines.

In a recent work by Zuchowska et al., they investigated the effect of shear stress on spheroids formed on a µSFC. They reported that high shear stresses (maximum of 0.9 dyne/cm^2) had adverse effects on forming cell aggregations and spheroid formation of A549 cell line while it did not affect MRC-5 cell spheroids [198]. According to their observations, A549 spheroids were formed more compactly in deep microwells (500 µm height) due to lower shear stresses in comparison with shallower ones (350 µm height). It is likely that the difference between the morphology of the cells is responsible for this outcome. In another work in which ovarian cancer cell spheroids were put under various shear stresses in a µSCC the authors claimed that under *in-vivo* relevant shear stresses similar to the condition in peritonium (<0.1 dyne/cm^2), the cancer cell spheroids showed higher chemoresistance and also exhibited a higher tendency towards tumorigenesis. In addition, it was shown that the cancer stem cells in the spheroids induced stem cell markers only under shear stress and not in static culture [186]. It can be concluded that the shear stress is a critical parameter in designing µSFCs and µSCCs as it affects cellular function and phenotype [199].

Creating geometries that generate low velocities and stagnation regions near spheroids leads to low shear stresses on cells [121]. In designing a µSCC, CFD analysis was performed to examine three different designs to optimize the geometry with respect to shear stress [89]. U-shaped microstructures and microwells also have the potential to be further refined with the aid of CFD analysis to limit shear stresses on cells [65]. For instance, the depth of microwells should be designed such that it is sufficient to protect spheroids from high shear stresses, particularly as they settle. Similarly, microwell diameters should be configured to ensure that spheroids do not exceed a specific size range [65]. Another way to protect multicellular spheroids from high shear stresses is to encapsulate them in hydrogel droplets [37]. In this way, the cells are not in direct contact with the main flow.

5.4. Cell loss

One drawback of most µSFCs is that cells may be lost during chip loading. This problem is more pronounced when the number of available cells is low, as is the case with primary cells and clinical samples. When cells are introduced at the inlet of the device, many of them do not trap within the chip. For instance, in most microwell-based µSFCs, cells that do not sediment within microwells are rinsed out with the flow of culture medium [6, 17, 40, 95, 125]. Therefore, many cells exit the device without taking part in the spheroid formation process. However, recent advances in µSFC design have resolved this issue [39, 88, 98, 155, 156, 200]. Gradually decreasing the depth of microwells can dramatically reduce the number of cell lost [39, 88, 135]. Using porous membranes for cell trapping is also useful [155, 156, 200]. Emulsion-based µSFCs do not usually allow cell loss since cells are encapsulated inside either the aqueous phase [149] or the hydrogel droplets [36].

5.5. Spheroid diameter and cell density

Various parameters influence spheroid diameter in a single µSFC. These include: cell type (Figure 15A); cell density (Figure 15B) [122, 125, 134]; microwell or microstructure

dimensions (Figure 15C and D) [7, 13, 125]; duration of cell seeding [39, 88, 98, 151]; and flow rate of the cell suspension [88, 98, 120].

In order to achieve desired diameters, one should take cell size into account. Patra *et al.* used different cell densities for HepG2 and COS-7 cell lines (10^7 and 10^5 cells/ml respectively), producing spheroid diameters of 200 µm and 80 µm, respectively [96]. This indicates that COS-7 cells are much larger than HepG2 cells. In another study, human glioma (U251) cells, human hepatocellular liver carcinoma (HepG2) cells, and human breast adenocarcinoma (MCF-7) cells were used to from spheroids using the same cell density of 5×10^6 cells/ml. However, the resulting spheroid sizes were considerably different, as shown in Figure 15A.

In a µSFC, cell density is a critical parameter responsible for spheroid size (Figure 15B). In microwell-based µSFCs, low cell densities lead to the formation of several small spheroids per well [17]. In contrast, excessive cell densities produce large and fragile aggregates that do not resemble spheroids. These loose aggregates lack spherical shape [185] and may clog microchannels [17]. Chen *et al.* investigated the effects of cell suspension density in a µSFC [134]. The authors reported that cell densities below 1×10^6 cells/ml led to compact spheroids after 24 hours, while a density of 2×10^6 cells/ml (for HCT116 cells) caused loose cell aggregates. Anada *et al.* reported similar results for cell densities above 4×10^6 cells/ml using HepG2 cells [185]. They also tried spheroid formation with a density of 8×10^6 cells/ml with the MG63 cell line and obtained compact spherical spheroids. These results show that the higher limit for cell density in a µSFC not only depends on the device design specifications but also on cell type.

Changing microwell dimensions is another way to generate different spheroid sizes from the same cell line (Figure 15C & D) [7, 125]. Patra *et al.* generated spheroids with diameters of 130 and 212 µm simply by adjusting the microwell dimensions [7]. The cross-sectional shapes of their microwells were squares with 200×200 µm and 300×300 µm dimensions (Figure 15C). Another design by Kim *et al.* allowed precise control on spheroid diameter by tuning three parameters simultaneously: flow rate, cell density, and duration of cell seeding [88, 135]. At equal cell seeding times, it is possible to increase cell density while lowering the flow rate and thereby obtain equivalent spheroid diameters. Sakai *et al.* reported that high culture medium flow rate increased the spheroid diameter by bringing the fresh medium and nutrients, and removing the waste products from the spheroid formation sites [201].

The addition of some factors can enhance the spheroid formation and its sphericity [202]. Increasing the fetal bovine serum (FBS) [163], reconstituted basement membrane (rBM) [48] or collagen [198] concentration in the culture media can enhance cell aggregation. Frey and co-workers investigated the effect of FBS concentration on spheroid formation of human colorectal carcinoma cells (HCT-116) in a µSFC. The authors reported that 0% concentration of FBS led to no spheroid formation while higher concentrations promoted larger diameter spheroids [163]. The spheroids produced from lung carcinoma cells (A-549 cell line) cultured on a µSFC were observed to improve sphericity and compaction only after the addition of collagen due to their low secretion of ECM proteins [198].

5.6. Methods of spheroid analysis

Evaluating and monitoring the spheroids before, during and after culturing and drug tests are crucial for interpreting the functionality of µSFCs and µSCCs. The monitoring methods are conducted off-chip or on-chip. Here, we briefly overview the off-chip techniques and then discuss the microfluidic designs to facilitate off-chip spheroid analysis. Finally, the recent advances in on-chip spheroid monitoring tools are elaborated.

5.6.1. Off-chip spheroid analysis methods and spheroid retrieval

Methods used conventionally for spheroid analysis can be categorized into two types. The first group needs spheroid retrieval which includes flow cytometry [7], scanning electron microscopy [36, 203, 204] and transmission electron microscopy [28]. The first group methods are typically conducted after the experiments and are solely endpoint assessment tools. The second group uses the supernatants collected from the outlet microchannels of the chip to evaluate the viability and metabolic activity of the cells after drug treatment [8, 39, 164] by conducting measurement of metabolites concentration, luminescence, and absorbance with the plate readers [39]. The supernatants contain caspase [8, 39], albumin [89], urea [40], glucose and lactate content [164] which can be used to determine the cellular apoptosis and functional conditions in the culture microenvironment on the chip. Parallelization is an option which can be considered to boost the total throughput for supernatants analysis which should be considered in the chip design. Although these methods are simple and easy to use, they are not efficient for online monitoring because the supernatant is usually extracted during the experiment and stored for later measurements.

The capacity to retrieve spheroids from µSFCs represents a significant capability, allowing researchers to obtain additional information about cell viability, apoptosis and necrosis using flow cytometry [7], or to distinguish differentiation states in the case of stem cells [189]. Accordingly, proper mechanisms for the retrieval of the spheroids are essential. Spheroid retrieval is facilitated by the careful design of microchannels, microwells, and microstructures on µSFCs. After spheroids are formed, they can be retrieved by reversing [16, 149] and/or increasing the flow rate [7, 96, 139], or by pneumatic actuation [119-121, 128, 185].

Mcmillan *et al.* [149] and Lee *et al.* [16] retrieved spheroids by reversing the flow direction in the device (Figure 16A and Figure 16B). The reversed flow exerts a higher pressure on spheroids in the opposite direction, forcing them to move back to the spheroid outlet. Several works including µSFCs [7, 96] and µSCCs [65, 139] retrieved spheroids by increasing the flow rate of the culture medium. They first simulated the flow field in square microwells to obtain the flow rate at which spheroids exit microwells due to hydrodynamic lift forces. Then, they applied this numerically obtained flow rate to their µSFC for spheroid retrieval. Xu *et al.* used two strategies for spheroid retrieval [125]. They either implemented high flow velocities (6 mm/sec) or inverted the device. As a result of the second technique, the spheroids could be retrieved with much lower fluid velocities (500 µm/sec). This method can reasonably reduce potential cell damage caused by high shear stress.

Recently, a number of pneumatics approaches has been utilized in µSFCs that allow spheroid retrieval. After spheroids are formed, and drug tests are completed, the pneumatically activated U-shaped barriers move downward, allowing spheroids to move towards the chip outlet [119, 120, 128] (Figure 16C). In a two-layered µSFC fabricated by Anada et al., the pressure inside the bottom channel was reduced to deform the membrane [185]. Thus, concave-bottomed microwells were formed as a result of the pressure difference across a thin, flexible PDMS membrane (Figure 16D). After spheroid formation, the pressure difference was set to zero such that concave-bottomed microwells reverted to a flat surface. Spheroids were then simply retrieved via pipetting.

In µSFCs or µSCCs lacking spheroid retrieval capacity, it is necessary to perform precise drug monitoring and screening on the chip. By turning the chip upside-down, Kang *et al.* developed a microfluidic platform that facilitated the formation and spontaneous differentiation of stem cell spheroids within microwells [189]. A flat area existed above each microwell on which spheroids fell. That area was pretreated with laminin and poly-$_L$-lysine to facilitate on-chip neuronal differentiation. Thus, while this device lacked spheroid retrieval

capacity, the need for spheroid retrieval was obviated by enabling on-chip differentiation and experimental monitoring.

5.6.2. On-chip spheroid analysis methods

Cellular viability and 3D morphology of the spheroids can be evaluated on-chip by using optical microscopy (Figure 16A(b) & A(c)) [120, 205], fluorescent microscopy (Figure 16A(b) & A(c)) [8, 105, 120], the non-destructive spectroscopic imaging [206], confocal microscopy [52, 105, 173] and scanning electrochemical microscopy (SECM) (Figure 7A) [151]. In on-chip live/dead fluorescent staining of the spheroids, the projected areas of green and red regions are quantified as live or dead portions of the spheroid following chemosensitivity tests. Non-fluorescent assessment of live/dead viability and sphericity of the spheroids [203] can be done using image processing software (e.g., ImageJ and MATLAB) by on-chip measuring the spheroid diameter every day as it changes as a result of cell proliferation or cell death [134].

Real-time monitoring of glucose consumption and lactate secretion of cell spheroids using electrode-based biosensors is implemented on an HD-based µSFC similar to the one shown in Figure 7G [207]. The electrodes were fabricated by metal deposition on a glass layer in the chip and were functionalized with a hydrogel coating containing lactate or glucose oxidase on them. The hanging droplets were in contact with hydrogels from their ceiling which enabled in situ monitoring of lactate (Figure 17A). The mentioned microfluidic HD concept was integrated into another work by Schmid *et al.* for electrical impedance spectroscopy [208]. Two pairs of platinum electrode inlays were deposited on a glass and placed in the HD culture similar to the previous design. The electrodes were placed lateral to the HD center in a way that each pair of them had various distances to it. Those placed farther were used for HD height measurements, and those placed closer to the center measured spheroid diameter size by quantifying the output current values for specific magnitudes of the applied voltage and signal. The measurements were based on the impedance changes of the HDs and spheroids due to their size and the resulting changes in the electrical field. Alexander *et al.* recently fabricated an on-chip platform for the measurement of extracellular acidification, oxygen uptake rate of cell spheroids, temperature and electrical impedance in a µSCC [209]. They pipetted the pre-formed spheroids into a 3D-printed cylindrical microwell in the chip which was confined with two membranes having 120 µm pores from the bottom and above (Figure 17A). The thin layered deposited microelectrodes were embedded below the microwell to measure the chamber pH and the oxygen consumption of HepG2 spheroids (Figure 17B). The device was coupled with a digital interface for user monitoring and automatic flow control of the chip. The non-invasive and label-free characteristics of these biosensors make them suitable tools for chemosensitivity monitoring and microenvironment control of cell spheroids in µSFCs and µSCCs.

6. Conclusions and future directions

In the present review, the application of microfluidics technology to the spheroid formation and culturing was discussed to illuminate its potential and benefits, as well as the challenges that remain relative to conventional cell culture methods. Various methods and techniques utilized in microfluidic spheroid formation and culture were described. These include microwells and U-shaped microstructures, the hydraulic-electric analogy, digital microfluidics and spheroid culture-only chips, as well as other creative designs related to µSFCs and µSCCs. In addition, the design considerations and affecting parameters relating to µSFCs and µSCCs were also discussed to provide a better understanding of the various parameters affecting on-chip spheroid formation and culture.

A common shortcoming among most of the existing µSFCs and µSCCs in the literature is their inability to facilitate high-throughput screening (HTS) in high-throughput spheroid formation (HTSF) devices. This deficiency needs to be addressed in future works. HTSF

needs a large number of microwells or microstructures to form numerous spheroids, while HTS requires the capacity to deliver different drug doses to each of those spheroids. Such drug delivery must occur within the microchannels on the chip, each having a specified concentration of the desired drug. Designing such a platform, despite being complex, would address the deficiencies of conventional HTS platforms such as multiwell or 384 hanging droplet (HD) plates. Methods and protocols for spheroid HTS have been devised using multiwell plates but unfortunately, retain the disadvantages of static cultures.

Despite advancements in the field of microfabrication, microfluidic platforms are intended to be used only once. In addition, since microfabrication processes are still considered expensive, using microfluidic drug screening platforms has not yet become common. Recent progress in 3D printing technology can be considered as a "killer application" in microfluidic cell culture platforms [210]. This technology enables rapid and inexpensive fabrication of various 3D microfluidic devices with complex integrated components. In addition, these microfluidic cell cultre devices can become much more efficient when used for HTS. This would facilitate easy handling and manipulation especially when the procedures can be carried out using automated and robot-actuated devices in biological laboratories. Using robotics for the handling of the µSFCs and µSCCs not only minimizes the human-made errors but also makes the procedure easier for the future end-users.

In most µSFCs and µSCCs, the capacity to retrieve the cultured multicellular spheroids is limited. Typically, either there is no possibility for spheroid retrieval or it requires high flow rates that can adversely affect cell viability. Thus, efficient spheroid retrieval is an essential factor that merits increased design focus for implementation in µSFCs and µSCCs. Integration of µSFCs and µSCCs with imaging tools is another way to better analyze cultured spheroids. Embedding microlenses within the microfluidic chip for online monitoring can be helpful in platforms where spheroid retrieval is not possible. On-chip spheroid monitoring and sensing with biosensors and spectrometry tools also are interesting subjects. The electrode-based biosensors recently conducted on µSFCs and µSCCs have shown encouraging results regarding their capability in measuring and controlling the culture microenvironment species concentrations such as lactate, glucose, oxygen and also giving the pH, electrical impedance and temperature in situ. It is predicted that by using these biosensors and coupling them with the user-friendly interfaces, these platforms will have entered the realm of commercialization.

One of the missing components in on-chip spheroid culture is the administration of mechanical stress on the spheroids to better mimic the *in-vivo* microenvironments. By integrating the µSFCs and µSCCs with micromechanical actuators, it will be possible to conduct chemosensitivity tests and expose the spheroid cells to the *in-vivo*-like extracellular forces. Another future direction which can be seen for on-chip spheroids culturing is the application of bioengineered scaffolds in the µSFCs and µSCCs. The scaffolds can provide suitable surroundings for the spheroids to recapitulate the neighboring tissues.

Introducing the non-spherical spheroids to the µSCCs is feasible because *in-vivo* tumors are not spheres per se. Thus, various *in-vivo* relevant geometries of cellular aggregates can be bioprinted off-chip and then introduced to a µSCC. By these cellular structures, some other aspects of the spheroids features will be explicitly revealed when these non-spherical shapes are also vascularized and consisted of various relevant cell types. Inevitably, these advances depend on the creation of more developed microfabrication and microfluidics techniques which are not out of reach in the near future.

While such advances represent essential directions for development, µSFCs and µSCCs have clearly shown their potential in 3D culture and drug screening. These devices have been keenly studied for over a decade, yet have not reached maturity and still need to become more robust and easy to handle. Their ability to mimic *in-vivo* microenvironments must still be improved to more closely recreate complex phenomena, such as angiogenesis and vascularization in oncology research. Excitingly, µSFC and µSCC development is now

accelerating, indicating that the impact of these platforms will continue to expand and advance across the biomedical research field.

Conflicts of Interest: The authors declare no conflict of interest.

Acknowledgments: N.K. would like to thank Dr. Saeid Marzbanrad for reading the manuscript and making insightful comments. K.M. would like to thank Mr. Ali Kamali for his useful English editing of the manuscript and Ms. Tina Moshksayan for preparing some of the figures.

References:

[1] F. Hirschhaeuser, H. Menne, C. Dittfeld, J. West, W. Mueller-Klieser, L.A. Kunz-Schughart, Multicellular tumor spheroids: an underestimated tool is catching up again, Journal of Biotechnology, 148(2010) 3-15.

[2] L.-B. Weiswald, D. Bellet, V. Dangles-Marie, Spherical cancer models in tumor biology, Neoplasia, 17(2015) 1-15.

[3] G. Mehta, A.Y. Hsiao, M. Ingram, G.D. Luker, S. Takayama, Opportunities and challenges for use of tumor spheroids as models to test drug delivery and efficacy, Journal of controlled release, 164(2012) 192-204.

[4] E. Fennema, N. Rivron, J. Rouwkema, C. van Blitterswijk, J. de Boer, Spheroid culture as a tool for creating 3D complex tissues, Trends in biotechnology, 31(2013) 108-15.

[5] B. Desoize, J.-C. Jardillier, Multicellular resistance: a paradigm for clinical resistance?, Critical reviews in oncology/hematology, 36(2000) 193-207.

[6] K. Kwapiszewska, A. Michalczuk, M. Rybka, R. Kwapiszewski, Z. Brzózka, A microfluidic-based platform for tumour spheroid culture, monitoring and drug screening, Lab on a Chip, 14(2014) 2096-104.

[7] B. Patra, C.-C. Peng, W.-H. Liao, C.-H. Lee, Y.-C. Tung, Drug testing and flow cytometry analysis on a large number of uniform sized tumor spheroids using a microfluidic device, Scientific reports, 6(2016) 21061.

[8] J. Ruppen, L. Cortes-Dericks, E. Marconi, G. Karoubi, R.A. Schmid, R. Peng, et al., A microfluidic platform for chemoresistive testing of multicellular pleural cancer spheroids, Lab on a Chip, 14(2014) 1198-205.

[9] A. Skardal, T. Shupe, A. Atala, Organoid-on-a-chip and body-on-a-chip systems for drug screening and disease modeling, Drug discovery today, 21(2016) 1399-411.

[10] K. Chen, M. Wu, F. Guo, P. Li, C.Y. Chan, Z. Mao, et al., Rapid formation of size-controllable multicellular spheroids via 3D acoustic tweezers, Lab on a Chip, 16(2016) 2636-43.

[11] T. Das, L. Meunier, L. Barbe, D. Provencher, O. Guenat, T. Gervais, et al., Empirical chemosensitivity testing in a spheroid model of ovarian cancer using a microfluidics-based multiplex platform, Biomicrofluidics, 7(2013) 011805.

[12] S. Agastin, U.-B.T. Giang, Y. Geng, L.A. DeLouise, M.R. King, Continuously perfused microbubble array for 3D tumor spheroid model, Biomicrofluidics, 5(2011) 024110.

[13] Y.-C. Chen, X. Lou, Z. Zhang, P. Ingram, E. Yoon, High-throughput cancer cell sphere formation for characterizing the efficacy of photo dynamic therapy in 3D cell cultures, Scientific reports, 5(2015) 12175.

[14] O. Trédan, C.M. Galmarini, K. Patel, I.F. Tannock, Drug resistance and the solid tumor microenvironment, Journal of the National Cancer Institute, 99(2007) 1441-54.

[15] C. Wang, Z. Tang, Y. Zhao, R. Yao, L. Li, W. Sun, Three-dimensional in vitro cancer models: a short review, Biofabrication, 6(2014) 022001.

[16] K. Lee, C. Kim, J.Y. Yang, H. Lee, B. Ahn, L. Xu, et al., Gravity-oriented microfluidic device for uniform and massive cell spheroid formation, Biomicrofluidics, 6(2012) 014114.

[17] K. Ziółkowska, A. Stelmachowska, R. Kwapiszewski, M. Chudy, A. Dybko, Z. Brzózka, Long-term three-dimensional cell culture and anticancer drug activity evaluation in a microfluidic chip, Biosensors and Bioelectronics, 40(2013) 68-74.

[18] L. Yu, M.C. Chen, K.C. Cheung, Droplet-based microfluidic system for multicellular tumor spheroid formation and anticancer drug testing, Lab on a Chip, 10(2010) 2424-32.

[19] N.R. Patel, B. Aryasomayajula, A.H. Abouzeid, V.P. Torchilin, Cancer cell spheroids for screening of chemotherapeutics and drug-delivery systems, Therapeutic delivery, 6(2015) 509-20.

[20] H. Moghadas, M.S. Saidi, N. Kashaninejad, N.-T. Nguyen, Challenge in particle delivery to cells in a microfluidic device, Drug Delivery and Translational Research, (2017) DOI: 10.1007/s13346-017-0467-3.

[21] R.Z. Lin, H.Y. Chang, Recent advances in three‐dimensional multicellular spheroid culture for biomedical research, Biotechnology journal, 3(2008) 1172-84.

[22] M. Ingram, G. Techy, R. Saroufeem, O. Yazan, K. Narayan, T. Goodwin, et al., Three-dimensional growth patterns of various human tumor cell lines in simulated microgravity of a NASA bioreactor, In Vitro Cellular & Developmental Biology-Animal, 33(1997) 459-66.

[23] J.A. Hickman, R. Graeser, R. de Hoogt, S. Vidic, C. Brito, M. Gutekunst, et al., Three‐dimensional models of cancer for pharmacology and cancer cell biology: Capturing tumor complexity in vitro/ex vivo, Biotechnology journal, 9(2014) 1115-28.

[24] S. Nath, G.R. Devi, Three-dimensional culture systems in cancer research: Focus on tumor spheroid model, Pharmacology & therapeutics, 163(2016) 94-108.

[25] V.E. Santo, M.F. Estrada, S.P. Rebelo, S. Abreu, I. Silva, C. Pinto, et al., Adaptable stirred-tank culture strategies for large scale production of multicellular spheroid-based tumor cell models, Journal of biotechnology, 221(2016) 118-29.

[26] J. Friedrich, R. Ebner, L.A. Kunz-Schughart, Experimental anti-tumor therapy in 3-D: spheroids–old hat or new challenge?, International journal of radiation biology, 83(2007) 849-71.

[27] E. Curcio, S. Salerno, G. Barbieri, L. De Bartolo, E. Drioli, A. Bader, Mass transfer and metabolic reactions in hepatocyte spheroids cultured in rotating wall gas-permeable membrane system, Biomaterials, 28(2007) 5487-97.

[28] J.M. Kelm, N.E. Timmins, C.J. Brown, M. Fussenegger, L.K. Nielsen, Method for generation of homogeneous multicellular tumor spheroids applicable to a wide variety of cell types, Biotechnology and bioengineering, 83(2003) 173-80.

[29] A.D. Conger, M.C. Ziskin, Growth of mammalian multicellular tumor spheroids, Cancer research, 43(1983) 556-60.

[30] R. Sutherland, R. Durand, Growth and cellular characteristics of multicell spheroids, Spheroids in cancer research, Springer1984, pp. 24-49.

[31] L.A. KUNZ‐SCHUGHART, M. Kreutz, R. Knuechel, Multicellular spheroids: a three-dimensional in vitro culture system to study tumour biology, International journal of experimental pathology, 79(1998) 1-23.

[32] N. Baek, O.W. Seo, M. Kim, J. Hulme, S.S.A. An, Monitoring the effects of doxorubicin on 3D-spheroid tumor cells in real-time, OncoTargets and therapy, 9(2016) 7207.

[33] G. Pettet, C. Please, M. Tindall, D. McElwain, The migration of cells in multicell tumor spheroids, Bulletin of mathematical biology, 63(2001) 231-57.

[34] J. Alvarez-Pérez, P. Ballesteros, S. Cerdán, Microscopic images of intraspheroidal pH by 1H magnetic resonance chemical shift imaging of pH sensitive indicators, Magnetic Resonance Materials in Physics, Biology and Medicine, 18(2005) 293-301.

[35] M.W. Laschke, M.D. Menger, Life is 3D: boosting spheroid function for tissue engineering, Trends in biotechnology, 35(2017) 133-44.

[36] P. Sabhachandani, V. Motwani, N. Cohen, S. Sarkar, V. Torchilin, T. Konry, Generation and functional assessment of 3D multicellular spheroids in droplet based microfluidics platform, Lab on a Chip, 16(2016) 497-505.

[37] A. Aung, J. Theprungsirikul, H.L. Lim, S. Varghese, Chemotaxis-driven assembly of endothelial barrier in a tumor-on-a-chip platform, Lab on a Chip, 16(2016) 1886-98.

[38] A.Y. Hsiao, Y.C. Tung, X. Qu, L.R. Patel, K.J. Pienta, S. Takayama, 384 hanging drop arrays give excellent Z‐factors and allow versatile formation of co‐culture spheroids, Biotechnology and Bioengineering, 109(2012) 1293-304.

[39] J. Ruppen, F.D. Wildhaber, C. Strub, S.R. Hall, R.A. Schmid, T. Geiser, et al., Towards personalized medicine: chemosensitivity assays of patient lung cancer cell spheroids in a perfused microfluidic platform, Lab on a Chip, 15(2015) 3076-85.

[40] S.-A. Lee, E. Kang, J. Ju, D.-S. Kim, S.-H. Lee, Spheroid-based three-dimensional liver-on-a-chip to investigate hepatocyte–hepatic stellate cell interactions and flow effects, Lab on a Chip, 13(2013) 3529-37.

[41] J.L. Allensworth, M.K. Evans, F. Bertucci, A.J. Aldrich, R.A. Festa, P. Finetti, et al., Disulfiram (DSF) acts as a copper ionophore to induce copper-dependent oxidative stress and mediate anti-tumor efficacy in inflammatory breast cancer, Molecular oncology, 9(2015) 1155-68.

[42] A. Faulkner-Jones, S. Greenhough, J.A. King, J. Gardner, A. Courtney, W. Shu, Development of a valve-based cell printer for the formation of human embryonic stem cell spheroid aggregates, Biofabrication, 5(2013) 015013.

[43] W.L. Haisler, D.M. Timm, J.A. Gage, H. Tseng, T. Killian, G.R. Souza, Three-dimensional cell culturing by magnetic levitation, Nature protocols, 8(2013) 1940-9.

[44] S.L. Ham, R. Joshi, G.D. Luker, H. Tavana, Engineered Breast Cancer Cell Spheroids Reproduce Biologic Properties of Solid Tumors, Advanced Healthcare Materials, 5(2016) 2788-98.

[45] C. Ingeson-Carlsson, A. Martinez-Monleon, M. Nilsson, Differential effects of MAPK pathway inhibitors on migration and invasiveness of BRAF V600E mutant thyroid cancer cells in 2D and 3D culture, Experimental cell research, 338(2015) 127-35.

[46] A.C. Lima, J.F. Mano, Micro/nano-structured superhydrophobic surfaces in the biomedical field: part II: applications overview, Nanomedicine, 10(2015) 271-97.

[47] M.B. Oliveira, A.I. Neto, C.R. Correia, M.I. Rial-Hermida, C. Alvarez-Lorenzo, J.o.F. Mano, Superhydrophobic chips for cell spheroids high-throughput generation and drug screening, ACS applied materials & interfaces, 6(2014) 9488-95.

[48] K. Shen, J. Lee, M.L. Yarmush, B. Parekkadan, Microcavity substrates casted from self-assembled microsphere monolayers for spheroid cell culture, Biomedical microdevices, 16(2014) 609-15.

[49] R.K. Vadivelu, C.H. Ooi, R.-Q. Yao, J.T. Velasquez, E. Pastrana, J. Diaz-Nido, et al., Generation of three-dimensional multiple spheroid model of olfactory ensheathing cells using floating liquid marbles, Scientific reports, 5(2015) 15083.

[50] J. Carlsson, J. Yuhas, Liquid-overlay culture of cellular spheroids, Spheroids in cancer research, Springer1984, pp. 1-23.

[51] V.N. Goral, S.H. Au, R.A. Faris, P.K. Yuen, Methods for advanced hepatocyte cell culture in microwells utilizing air bubbles, Lab on a Chip, 15(2015) 1032-7.

[52] A. Neto, C. Correia, M. Oliveira, M. Rial-Hermida, C. Alvarez-Lorenzo, R. Reis, et al., A novel hanging spherical drop system for the generation of cellular spheroids and high throughput combinatorial drug screening, Biomaterials Science, 3(2015) 581-5.

[53] S.L. Nyberg, J. Hardin, B. Amiot, U.A. Argikar, R.P. Remmel, P. Rinaldo, Rapid, large ‐ scale formation of porcine hepatocyte spheroids in a novel spheroid reservoir bioartificial liver, Liver transplantation, 11(2005) 901-10.

[54] Y.-C. Tung, A.Y. Hsiao, S.G. Allen, Y.-s. Torisawa, M. Ho, S. Takayama, High-throughput 3D spheroid culture and drug testing using a 384 hanging drop array, Analyst, 136(2011) 473-8.

[55] E.J. Vrij, S. Espinoza, M. Heilig, A. Kolew, M. Schneider, C. van Blitterswijk, et al., 3D high throughput screening and profiling of embryoid bodies in thermoformed microwell plates, Lab on a Chip, 16(2016) 734-42.

[56] M. Chatzinikolaidou, Cell spheroids: the new frontiers in in vitro models for cancer drug validation, Drug Discovery Today, 21(2016) 1553-60.

[57] E.W. Young, Cells, tissues, and organs on chips: challenges and opportunities for the cancer tumor microenvironment, Integrative Biology, 5(2013) 1096-109.

[58] H. Hwang, J. Park, C. Shin, Y. Do, Y.-K. Cho, Three dimensional multicellular co-cultures and anti-cancer drug assays in rapid prototyped multilevel microfluidic devices, Biomedical Microdevices, 15(2013) 627-34.

[59] N.-T. Nguyen, M. Hejazian, C.H. Ooi, N. Kashaninejad, Recent Advances and Future Perspectives on Microfluidic Liquid Handling, Micromachines, 8(2017) 186.

[60] N.-T. Nguyen, S.A.M. Shaegh, N. Kashaninejad, D.-T. Phan, Design, fabrication and characterization of drug delivery systems based on lab-on-a-chip technology, Advanced Drug Delivery Reviews, 65(2013) 1403-19.

[61] S.M.A. Mortazavi, P. Tirandazi, M. Normandie, M.S. Saidi, Efficient batch-mode mixing and flow patterns in a microfluidic centrifugal platform: a numerical and experimental study, Microsystem Technologies, 23(2017) 2767-79.

[62] S. Ghadami, R. Kowsari-Esfahan, M.S. Saidi, K. Firoozbakhsh, Spiral microchannel with stair-like cross section for size-based particle separation, Microfluidics and Nanofluidics, 21(2017) 115.

[63] G. Hu, D. Li, Three-dimensional modeling of transport of nutrients for multicellular tumor spheroid culture in a microchannel, Biomedical microdevices, 9(2007) 315-23.

[64] K. Moshksayan, N. Kashaninejad, M.S. Saidi, Mathematical Analysis of a Conventional Microfluidic Device Culturing Tumor Spheroids, International Congress on Cancer Prevention & Early Detection Integration of Research & Action, Archives of Iranian Medicine, Tehran, Iran, 2017.

[65] N. Rousset, F. Monet, T. Gervais, Simulation-assisted design of microfluidic sample traps for optimal trapping and culture of non-adherent single cells, tissues, and spheroids, Scientific Reports, 7(2017) 245.

[66] K. Moshksayan, N. Kashaninejad, M.S. Saidi, Numerical investigation of the effects of functional parameters in hypoxia initiation within a cell spheroid cultured in a microfluidic chip, 25th Annual International Conference on Mechanical Engineering held by ISME Tehran, Iran, 2017, pp. 861-2.

[67] F. Nejadnasrollah, B. Firoozabadi, Selection and simulation of a proper microfluidic for hepatocyte culture, Biomedical Engineering (ICBME), 2015 22nd Iranian Conference on, IEEE2015, pp. 65-9.

[68] Y.Y. Choi, J. Kim, S.-H. Lee, D.-S. Kim, Lab on a chip-based hepatic sinusoidal system simulator for optimal primary hepatocyte culture, Biomedical microdevices, 18(2016) 1-9.

[69] B. Larson, 3D Cell Culture: A Review of Current Techniques, (2015).

[70] T.-M. Achilli, J. Meyer, J.R. Morgan, Advances in the formation, use and understanding of multi-cellular spheroids, Expert opinion on biological therapy, 12(2012) 1347-60.

[71] S. Breslin, L. O'Driscoll, Three-dimensional cell culture: the missing link in drug discovery, Drug discovery today, 18(2013) 240-9.

[72] D.V. LaBarbera, B.G. Reid, B.H. Yoo, The multicellular tumor spheroid model for high-throughput cancer drug discovery, Expert opinion on drug discovery, 7(2012) 819-30.

[73] R.K. Vadivelu, H. Kamble, M.J. Shiddiky, N.-T. Nguyen, Microfluidic Technology for the Generation of Cell Spheroids and Their Applications, Micromachines, 8(2017) 94.

[74] D. Pappas, Microfluidics and cancer analysis: cell separation, cell/tissue culture, cell mechanics, and integrated analysis systems, Analyst, 141(2016) 525-35.

[75] N. Kashaninejad, M.R. Nikmaneshi, H. Moghadas, A. Kiyoumarsi Oskouei, M. Rismanian, M. Barisam, et al., Organ-Tumor-on-a-Chip for Chemosensitivity Assay: A Critical Review, Micromachines, 7(2016) 130.

[76] P.K. Chaudhuri, M.E. Warkiani, T. Jing, C.T. Lim, Microfluidics for research and applications in oncology, Analyst, 141(2016) 504-24.

[77] A. Boussommier-Calleja, R. Li, M.B. Chen, S.C. Wong, R.D. Kamm, Microfluidics: a new tool for modeling cancer–immune interactions, Trends in cancer, 2(2016) 6-19.

[78] H.-C. Chang, C.-Y. Tang, H.-Y. Lin, C.-H. Hsu, Microfluidic Tumor-mimicking In Vitro Cell Culture Methods, International Journal of Automation and Smart Technology, 6(2016) 211-6.

[79] K.E. Sung, D.J. Beebe, Microfluidic 3D models of cancer, Advanced drug delivery reviews, 79(2014) 68-78.

[80] Y.S. Zhang, Y.-N. Zhang, W. Zhang, Cancer-on-a-chip systems at the frontier of nanomedicine, Drug Discovery Today, (2017).

[81] N. Gupta, J.R. Liu, B. Patel, D.E. Solomon, B. Vaidya, V. Gupta, Microfluidics - based 3D cell culture models: Utility in novel drug discovery and delivery research, Bioengineering & Translational Medicine, 1(2016) 63-81.

[82] R. Li, X. Lv, X. Zhang, O. Saeed, Y. Deng, Microfluidics for cell-cell interactions: A review, Frontiers of Chemical Science and Engineering, 10(2016) 90-8.

[83] V. van Duinen, S.J. Trietsch, J. Joore, P. Vulto, T. Hankemeier, Microfluidic 3D cell culture: from tools to tissue models, Current opinion in biotechnology, 35(2015) 118-26.

[84] G. Du, Q. Fang, J.M. den Toonder, Microfluidics for cell-based high throughput screening platforms—A review, Analytica chimica acta, 903(2016) 36-50.

[85] X.J. Li, A.V. Valadez, P. Zuo, Z. Nie, Microfluidic 3D cell culture: potential application for tissue-based bioassays, (2012).

[86] Y. Morimoto, S. Takeuchi, Three-dimensional cell culture based on microfluidic techniques to mimic living tissues, Biomaterials Science, 1(2013) 257-64.

[87] A. Munaz, R.K. Vadivelu, J.A. St John, N.-T. Nguyen, A lab-on-a-chip device for investigating the fusion process of olfactory ensheathing cell spheroids, Lab on a Chip, 16(2016) 2946-54.

[88] C. Kim, J.H. Bang, Y.E. Kim, S.H. Lee, J.Y. Kang, On-chip anticancer drug test of regular tumor spheroids formed in microwells by a distributive microchannel network, Lab on a chip, 12(2012) 4135-42.

[89] J.-Y. Kim, D.A. Fluri, R. Marchan, K. Boonen, S. Mohanty, P. Singh, et al., 3D spherical microtissues and microfluidic technology for multi-tissue experiments and analysis, Journal of biotechnology, 205(2015) 24-35.

[90] L. Aoun, P. Weiss, A. Laborde, B. Ducommun, V. Lobjois, C. Vieu, Microdevice arrays of high aspect ratio poly (dimethylsiloxane) pillars for the investigation of multicellular tumour spheroid mechanical properties, Lab on a Chip, 14(2014) 2344-53.

[91] S. Halldorsson, E. Lucumi, R. Gómez-Sjöberg, R.M. Fleming, Advantages and challenges of microfluidic cell culture in polydimethylsiloxane devices, Biosensors and Bioelectronics, 63(2015) 218-31.

[92] S.A. Mousavi Shaegh, F. De Ferrari, Y.S. Zhang, M. Nabavinia, N. Binth Mohammad, J. Ryan, et al., A microfluidic optical platform for real-time monitoring of pH and oxygen in microfluidic bioreactors and organ-on-chip devices, Biomicrofluidics, 10(2016) 044111.

[93] R. Riahi, S.A.M. Shaegh, M. Ghaderi, Y.S. Zhang, S.R. Shin, J. Aleman, et al., Automated microfluidic platform of bead-based electrochemical immunosensor integrated with bioreactor for continual monitoring of cell secreted biomarkers, Scientific reports, 6(2016).

[94] P. Tabeling, Introduction to Microfluidics, Great Britain: Oxford University Press Inc.; 2005.

[95] K. Ziółkowska, R. Kwapiszewski, A. Stelmachowska, M. Chudy, A. Dybko, Z. Brzózka, Development of a three-dimensional microfluidic system for long-term tumor spheroid culture, Sensors and Actuators B: Chemical, 173(2012) 908-13.

[96] B. Patra, Y.-H. Chen, C.-C. Peng, S.-C. Lin, C.-H. Lee, Y.-C. Tung, A microfluidic device for uniform-sized cell spheroids formation, culture, harvesting and flow cytometry analysis, Biomicrofluidics, 7(2013) 054114.

[97] N. Kashaninejad, N.-T. Nguyen, W.K. Chan, The three-phase contact line shape and eccentricity effect of anisotropic wetting on hydrophobic surfaces, Soft Matter, 9(2013) 527-35.

[98] C. Kim, S. Chung, Y.E. Kim, K.S. Lee, S.H. Lee, K.W. Oh, et al., Generation of core-shell microcapsules with three-dimensional focusing device for efficient formation of cell spheroid, Lab on a Chip, 11(2011) 246-52.

[99] S. Hong, H.-J. Hsu, R. Kaunas, J. Kameoka, Collagen microsphere production on a chip, Lab on a Chip, 12(2012) 3277-80.

[100] Y. Wang, L. Zhao, C. Tian, C. Ma, J. Wang, Geometrically controlled preparation of various cell aggregates by droplet-based microfluidics, Analytical Methods, 7(2015) 10040-51.

[101] K. Alessandri, B.R. Sarangi, V.V. Gurchenkov, B. Sinha, T.R. Kießling, L. Fetler, et al., Cellular capsules as a tool for multicellular spheroid production and for investigating the mechanics of tumor progression in vitro, Proceedings of the National Academy of Sciences, 110(2013) 14843-8.

[102] H.F. Chan, Y. Zhang, Y.-P. Ho, Y.-L. Chiu, Y. Jung, K.W. Leong, Rapid formation of multicellular spheroids in double-emulsion droplets with controllable microenvironment, Scientific reports, 3(2013).

[103] K.S. McMillan, A.G. McCluskey, A. Sorensen, M. Boyd, M. Zagnoni, Emulsion technologies for multicellular tumour spheroid radiation assays, Analyst, 141(2016) 100-10.

[104] R. Tomasi, G. Amselem, C.N. Baroud, High density hydrogel arrays for 3d cell colonies with dynamically controlled external stimuli, International Conference on Miniaturized Systems for Chemistry and Life Sciences, Freiburg, Germany, 2013.

[105] S. Yoon, J.A. Kim, S.H. Lee, M. Kim, T.H. Park, Droplet-based microfluidic system to form and separate multicellular spheroids using magnetic nanoparticles, Lab on a Chip, 13(2013) 1522-8.

[106] C.H. Schmitz, A.C. Rowat, S. Köster, D.A. Weitz, Dropspots: a picoliter array in a microfluidic device, Lab on a Chip, 9(2009) 44-9.

[107] Y. Wang, J. Wang, Mixed hydrogel bead-based tumor spheroid formation and anticancer drug testing, Analyst, 139(2014) 2449-58.

[108] L. Yu, C. Ni, S.M. Grist, C. Bayly, K.C. Cheung, Alginate core-shell beads for simplified three-dimensional tumor spheroid culture and drug screening, Biomedical microdevices, 17(2015) 1-9.

[109] S. Mashaghi, A. Abbaspourrad, D.A. Weitz, A.M. van Oijen, Droplet microfluidics: A tool for biology, chemistry and nanotechnology, TrAC Trends in Analytical Chemistry, 82(2016) 118-25.

[110] G. Helmlinger, P.A. Netti, H.C. Lichtenbeld, R.J. Melder, R.K. Jain, Solid stress inhibits the growth of multicellular tumor spheroids, Nature biotechnology, 15(1997) 778-83.

[111] D.M. Hall, S.A. Brooks, In Vitro Invasion Assay Using Matrigel™: A Reconstituted Basement Membrane Preparation, Metastasis Research Protocols, (2014) 1-11.

[112] L. Yu, C. Bayly, K. Cheung, C, Matrigel-alginate core-shell beads for controlled tumor spheroid formation The 17th International Conference on Miniaturized Systems for Chemistry and Life Sciences, Freiburg, Germany, 2013, pp. 1716–8.

[113] L. Yao, F. Phan, Y. Li, Collagen microsphere serving as a cell carrier supports oligodendrocyte progenitor cell growth and differentiation for neurite myelination in vitro, Stem cell research & therapy, 4(2013) 109.

[114] A.C. Lima, J.F. Mano, A. Concheiro, C. Alvarez-Lorenzo, Fast and mild strategy, using superhydrophobic surfaces, to produce collagen/platelet lysate gel beads for skin regeneration, Stem Cell Reviews and Reports, 11(2015) 161-79.

[115] Y. Li, H. Cheng, K. Cheung, D. Chan, B. Chan, Mesenchymal stem cell-collagen microspheres for articular cartilage repair: cell density and differentiation status, Acta biomaterialia, 10(2014) 1919-29.

[116] Y.Y. Li, H.J. Diao, T.K. Chik, C.T. Chow, X.M. An, V. Leung, et al., Delivering mesenchymal stem cells in collagen microsphere carriers to rabbit degenerative disc: reduced risk of osteophyte formation, Tissue Engineering Part A, 20(2014) 1379-91.

[117] S. Sugiura, T. Oda, Y. Aoyagi, R. Matsuo, T. Enomoto, K. Matsumoto, et al., Microfabricated airflow nozzle for microencapsulation of living cells into 150 micrometer microcapsules, Biomedical microdevices, 9(2007) 91-9.

[118] C.-Y. Fu, S.-Y. Tseng, S.-M. Yang, L. Hsu, C.-H. Liu, H.-Y. Chang, A microfluidic chip with a U-shaped microstructure array for multicellular spheroid formation, culturing and analysis, Biofabrication, 6(2014) 015009.

[119] H.-J. Jin, Y.-H. Cho, J.-M. Gu, J. Kim, Y.-S. Oh, A multicellular spheroid formation and extraction chip using removable cell trapping barriers, Lab on a Chip, 11(2010) 115-9.

[120] W. Liu, J. Xu, T. Li, L. Zhao, C. Ma, S. Shen, et al., Monitoring Tumor Response to Anticancer Drugs Using Stable Three-Dimensional Culture in a Recyclable Microfluidic Platform, Analytical chemistry, 87(2015) 9752-60.

[121] L.Y. Wu, D. Di Carlo, L.P. Lee, Microfluidic self-assembly of tumor spheroids for anticancer drug discovery, Biomedical microdevices, 10(2008) 197-202.

[122] H. Ota, N. Miki, Microfluidic experimental platform for producing size-controlled three-dimensional spheroids, Sensors and Actuators A: Physical, 169(2011) 266-73.

[123] H. Ota, R. Yamamoto, K. Deguchi, Y. Tanaka, Y. Kazoe, Y. Sato, et al., Three-dimensional spheroid-forming lab-on-a-chip using micro-rotational flow, Sensors and Actuators B: Chemical, 147(2010) 359-65.

[124] J. Fukuda, K. Nakazawa, Hepatocyte spheroid arrays inside microwells connected with microchannels, Biomicrofluidics, 5(2011) 022205.

[125] Y. Xu, F. Xie, T. Qiu, L. Xie, W. Xing, J. Cheng, Rapid fabrication of a microdevice with concave microwells and its application in embryoid body formation, Biomicrofluidics, 6(2012) 016504.

[126] M. Barisam, N. Kashaninejad, M.S. Saidi, N.-T. Nguyen, Prediction of necrotic core and hypoxic zone of multicellular spheroids in a microbioreactor, Micromachines, (2018) Under Review.

[127] M. Barisam, M.S. Saidi, N. Kashaninejad, R. Vadivelu, N.-T. Nguyen, Numerical simulation of the behavior of toroidal and spheroidal multicellular aggregates in microfluidic devices with microwell and U-shaped barrier, Micromachines, 8(2017) 358.

[128] W. Liu, J.-C. Wang, J. Wang, Controllable organization and high throughput production of recoverable 3D tumors using pneumatic microfluidics, Lab on a Chip, 15(2015) 1195-204.

[129] B. Zhang, M.-C. Kim, T. Thorsen, Z. Wang, A self-contained microfluidic cell culture system, Biomedical microdevices, 11(2009) 1233-7.

[130] M.-C. Kim, Z. Wang, R.H. Lam, T. Thorsen, Building a better cell trap: Applying Lagrangian modeling to the design of microfluidic devices for cell biology, Journal of applied physics, 103(2008) 044701.

[131] T. Anada, J. Fukuda, Y. Sai, O. Suzuki, An oxygen-permeable spheroid culture system for the prevention of central hypoxia and necrosis of spheroids, Biomaterials, 33(2012) 8430-41.

[132] J. Fukuda, K. Nakazawa, Orderly arrangement of hepatocyte spheroids on a microfabricated chip, Tissue engineering, 11(2005) 1254-62.

[133] T. Okuyama, H. Yamazoe, N. Mochizuki, A. Khademhosseini, H. Suzuki, J. Fukuda, Preparation of arrays of cell spheroids and spheroid-monolayer cocultures within a microfluidic device, Journal of bioscience and bioengineering, 110(2010) 572-6.

[134] Y. Chen, D. Gao, H. Liu, S. Lin, Y. Jiang, Drug cytotoxicity and signaling pathway analysis with three-dimensional tumor spheroids in a microwell-based microfluidic chip for drug screening, Analytica chimica acta, 898(2015) 85-92.

[135] C. Kim, K.S. Lee, J.H. Bang, Y.E. Kim, M.-C. Kim, K.W. Oh, et al., 3-Dimensional cell culture for on-chip differentiation of stem cells in embryoid body, Lab on a Chip, 11(2011) 874-82.

[136] H.E. Abaci, R. Devendra, Q. Smith, S. Gerecht, G. Drazer, Design and development of microbioreactors for long-term cell culture in controlled oxygen microenvironments, Biomedical microdevices, 14(2012) 145-52.

[137] C.R. Ethier, C.A. Simmons, Introductory biomechanics: from cells to organisms: Cambridge University Press; 2007.

[138] A. Aleksandrova, N. Pulkova, T. Gerasimenko, N.Y. Anisimov, S. Tonevitskaya, D. Sakharov, Mathematical and Experimental Model of Oxygen Diffusion for HepaRG Cell Spheroids, Bulletin of experimental biology and medicine, 160(2016) 857-60.

[139] M. Astolfi, B. Péant, M. Lateef, N. Rousset, J. Kendall-Dupont, E. Carmona, et al., Micro-dissected tumor tissues on chip: an ex vivo method for drug testing and personalized therapy, Lab on a Chip, 16(2016) 312-25.

[140] D.R. Grimes, C. Kelly, K. Bloch, M. Partridge, A method for estimating the oxygen consumption rate in multicellular tumour spheroids, Journal of The Royal Society Interface, 11(2014) 20131124.

[141] A. Zuchowska, K. Kwapiszewska, M. Chudy, A. Dybko, Z. Brzozka, Studies of anticancer drug cytotoxicity based on long‐term HepG2 spheroid culture in a microfluidic system, Electrophoresis, (2017).

[142] K.W. Oh, K. Lee, B. Ahn, E.P. Furlani, Design of pressure-driven microfluidic networks using electric circuit analogy, Lab on a Chip, 12(2012) 515-45.

[143] N. Kashaninejad, N.-T. Nguyen, W.K. Chan, Eccentricity effects of microhole arrays on drag reduction efficiency of microchannels with a hydrophobic wall, Physics of Fluids, 24(2012) 112004.

[144] N. Kashaninejad, W. Kong Chan, N.-T. Nguyen, Analytical Modeling of Slip Flow in Parallel-plate Microchannels, Micro and Nanosystems, 5(2013) 245-52.

[145] N. Kashaninejad, W.K. Chan, N.-T. Nguyen, Fluid mechanics of flow through rectangular hydrophobic microchannels, ASME 2011 9th International Conference on Nanochannels, Microchannels, and Minichannels, American Society of Mechanical Engineers, Edmonton, AL, Canada, 2011, pp. 647-55.

[146] Y.A. Cengel, Fluid mechanics: Tata McGraw-Hill Education; 2010.

[147] F.M. White, Fluid Mechanics, 7th ed.: Mcgraw-Hill; 2009.

[148] W.-H. Tan, S. Takeuchi, A trap-and-release integrated microfluidic system for dynamic microarray applications, Proceedings of the National Academy of Sciences, 104(2007) 1146-51.

[149] K.S. McMillan, M. Boyd, M. Zagnoni, Transitioning from multi-phase to single-phase microfluidics for long-term culture and treatment of multicellular spheroids, Lab on a Chip, (2016).

[150] A. Ahmad Khalili, M.R. Ahmad, M. Takeuchi, M. Nakajima, Y. Hasegawa, R. Mohamed Zulkifli, A Microfluidic Device for Hydrodynamic Trapping and Manipulation Platform of a Single Biological Cell, Applied Sciences, 6(2016) 40.

[151] Y.-s. Torisawa, A. Takagi, Y. Nashimoto, T. Yasukawa, H. Shiku, T. Matsue, A multicellular spheroid array to realize spheroid formation, culture, and viability assay on a chip, Biomaterials, 28(2007) 559-66.

[152] H. Ota, T. Kodama, N. Miki, Rapid formation of size-controlled three dimensional hetero-cell aggregates using micro-rotation flow for spheroid study, Biomicrofluidics, 5(2011) 034105.

[153] S.-M. Ong, C. Zhang, Y.-C. Toh, S.H. Kim, H.L. Foo, C.H. Tan, et al., A gel-free 3D microfluidic cell culture system, Biomaterials, 29(2008) 3237-44.

[154] S.R. Yazdi, A. Shadmani, S.C. Bürgel, P.M. Misun, A. Hierlemann, O. Frey, Adding the 'heart'to hanging drop networks for microphysiological multi-tissue experiments, Lab on a Chip, 15(2015) 4138-47.

[155] C.-T. Kuo, C.-L. Chiang, R.Y.-J. Huang, H. Lee, A.M. Wo, Configurable 2D and 3D spheroid tissue cultures on bioengineered surfaces with acquisition of epithelial–mesenchymal transition characteristics, NPG Asia Materials, 4(2012) e27.

[156] A.Y. Hsiao, Y.-s. Torisawa, Y.-C. Tung, S. Sud, R.S. Taichman, K.J. Pienta, et al., Microfluidic system for formation of PC-3 prostate cancer co-culture spheroids, Biomaterials, 30(2009) 3020-7.

[157] Y.-s. Torisawa, B.-h. Chueh, D. Huh, P. Ramamurthy, T.M. Roth, K.F. Barald, et al., Efficient formation of uniform-sized embryoid bodies using a compartmentalized microchannel device, Lab on a Chip, 7(2007) 770-6.

[158] H. Moghadas, M.S. Saidi, N. Kashaninejad, A. Kiyoumarsioskouei, N.-T. Nguyen, Fabrication and characterization of low-cost, bead-free, durable and hydrophobic electrospun membrane for 3D cell culture, Biomedical Microdevices, 19(2017) 74.

[159] C.S. Shin, B. Kwak, B. Han, K. Park, Development of an in vitro 3D tumor model to study therapeutic efficiency of an anticancer drug, Molecular pharmaceutics, 10(2013) 2167-75.

[160] Y.-C. Toh, C. Zhang, J. Zhang, Y.M. Khong, S. Chang, V.D. Samper, et al., A novel 3D mammalian cell perfusion-culture system in microfluidic channels, Lab on a Chip, 7(2007) 302-9.

[161] G.M. Keller, In vitro differentiation of embryonic stem cells, Current opinion in cell biology, 7(1995) 862-9.

[162] Y.S. Heo, L.M. Cabrera, J.W. Song, N. Futai, Y.-C. Tung, G.D. Smith, et al., Characterization and resolution of evaporation-mediated osmolality shifts that constrain microfluidic cell culture in poly (dimethylsiloxane) devices, Analytical chemistry, 79(2007) 1126-34.

[163] O. Frey, P.M. Misun, D.A. Fluri, J.G. Hengstler, A. Hierlemann, Reconfigurable microfluidic hanging drop network for multi-tissue interaction and analysis, Nature communications, 5(2014).

[164] I. Maschmeyer, A.K. Lorenz, K. Schimek, T. Hasenberg, A.P. Ramme, J. Hübner, et al., A four-organ-chip for interconnected long-term co-culture of human intestine, liver, skin and kidney equivalents, Lab on a Chip, 15(2015) 2688-99.

[165] S. Bauer, C.W. Huldt, K.P. Kanebratt, I. Durieux, D. Gunne, S. Andersson, et al., Functional coupling of human pancreatic islets and liver spheroids on-a-chip: Towards a novel human ex vivo type 2 diabetes model, Scientific Reports, 7(2017) 14620.

[166] M. Abdelgawad, A.R. Wheeler, The digital revolution: a new paradigm for microfluidics, Advanced Materials, 21(2009) 920-5.

[167] K. Choi, A.H. Ng, R. Fobel, A.R. Wheeler, Digital microfluidics, Annual review of analytical chemistry, 5(2012) 413-40.

[168] C.H. Ooi, A. Van Nguyen, G.M. Evans, O. Gendelman, E. Bormashenko, N.-T. Nguyen, A floating self-propelling liquid marble containing aqueous ethanol solutions, RSC Advances, 5(2015) 101006-12.

[169] A.A. García, A. Egatz-Gómez, S.A. Lindsay, P. Dominguez-Garcia, S. Melle, M. Marquez, et al., Magnetic movement of biological fluid droplets, Journal of Magnetism and Magnetic Materials, 311(2007) 238-43.

[170] M.K. Khaw, C.H. Ooi, F. Mohd-Yasin, R. Vadivelu, J. St John, N.-T. Nguyen, Digital microfluidics with a magnetically actuated floating liquid marble, Lab on a Chip, 16(2016) 2211-8.

[171] S.-Y. Park, M.A. Teitell, E.P. Chiou, Single-sided continuous optoelectrowetting (SCOEW) for droplet manipulation with light patterns, Lab on a Chip, 10(2010) 1655-61.

[172] S.H. Au, M.D. Chamberlain, S. Mahesh, M.V. Sefton, A.R. Wheeler, Hepatic organoids for microfluidic drug screening, Lab on a Chip, 14(2014) 3290-9.

[173] B.F. Bender, A.P. Aijian, R.L. Garrell, Digital microfluidics for spheroid-based invasion assays, Lab on a Chip, 16(2016) 1505-13.

[174] D. Bogojevic, M.D. Chamberlain, I. Barbulovic-Nad, A.R. Wheeler, A digital microfluidic method for multiplexed cell-based apoptosis assays, Lab on a Chip, 12(2012) 627-34.

[175] N. Kashaninejad, M.J.A. Shiddiky, N.-T. Nguyen, Advances in microfluidics-based assisted reproductive technology: from sperm sorter to reproductive system-on-a-chip Advanced Biosystems, In press(2018) DOI: 10.1002/adbi.201700197.

[176] I. Barbulovic-Nad, S.H. Au, A.R. Wheeler, A microfluidic platform for complete mammalian cell culture, Lab on a Chip, 10(2010) 1536-42.

[177] S. Srigunapalan, I.A. Eydelnant, C.A. Simmons, A.R. Wheeler, A digital microfluidic platform for primary cell culture and analysis, Lab on a Chip, 12(2012) 369-75.

[178] I.A. Eydelnant, B.B. Li, A.R. Wheeler, Microgels on-demand, Nature communications, 5(2014).

[179] A.H. Ng, B.B. Li, M.D. Chamberlain, A.R. Wheeler, Digital microfluidic cell culture, Annual review of biomedical engineering, 17(2015) 91-112.

[180] A.P. Aijian, R.L. Garrell, Digital microfluidics for automated hanging drop cell spheroid culture, Journal of laboratory automation, 20(2015) 283-95.

[181] I.A. Eydelnant, B.B. Li, A.R. Wheeler, Virtual microwells for three-dimensional cell culture on a digital microfluidic platform, IEEE 25th International Conference on Micro Electro Mechanical Systems (MEMS), IEEE2012, pp. 898-901.

[182] I.A. Eydelnant, U. Uddayasankar, B.B. Li, M.W. Liao, A.R. Wheeler, Virtual microwells for digital microfluidic reagent dispensing and cell culture, Lab on a Chip, 12(2012) 750-7.

[183] A. Zuchowska, E. Jastrzebska, M. Chudy, A. Dybko, Z. Brzozka, 3D lung spheroid cultures for evaluation of photodynamic therapy (PDT) procedures in microfluidic Lab-on-a-Chip system, Analytica chimica acta, 990(2017) 110-20.

[184] K. Hribar, D. Finlay, X. Ma, X. Qu, M. Ondeck, P. Chung, et al., Nonlinear 3D projection printing of concave hydrogel microstructures for long-term multicellular spheroid and embryoid body culture, Lab on a Chip, 15(2015) 2412-8.

[185] T. Anada, T. Masuda, Y. Honda, J. Fukuda, F. Arai, T. Fukuda, et al., Three-dimensional cell culture device utilizing thin membrane deformation by decompression, Sensors and Actuators B: Chemical, 147(2010) 376-9.

[186] C.K. Ip, S.-S. Li, M.Y. Tang, S.K. Sy, Y. Ren, H.C. Shum, et al., Stemness and chemoresistance in epithelial ovarian carcinoma cells under shear stress, Scientific reports, 6(2016) 26788.

[187] C.K. Byun, K. Abi‐Samra, Y.K. Cho, S. Takayama, Pumps for microfluidic cell culture, Electrophoresis, 35(2014) 245-57.

[188] S.A.M. Shaegh, Z. Wang, S.H. Ng, R. Wu, H.T. Nguyen, L.C.Z. Chan, et al., Plug-and-play microvalve and micropump for rapid integration with microfluidic chips, Microfluidics and Nanofluidics, 19(2015) 557-64.

[189] E. Kang, Y.Y. Choi, Y. Jun, B.G. Chung, S.-H. Lee, Development of a multi-layer microfluidic array chip to culture and replate uniform-sized embryoid bodies without manual cell retrieval, Lab on a Chip, 10(2010) 2651-4.

[190] E. Berthier, D.J. Beebe, Flow rate analysis of a surface tension driven passive micropump, Lab on a Chip, 7(2007) 1475-8.

[191] L.J.Y. Ong, L.H. Chong, L. Jin, P.K. Singh, P.S. Lee, H. Yu, et al., A pump‐free microfluidic 3D perfusion platform for the efficient differentiation of human hepatocyte‐like cells, Biotechnology and Bioengineering, (2017).

[192] J.Y. Park, C.M. Hwang, S.H. Lee, S.-H. Lee, Gradient generation by an osmotic pump and the behavior of human mesenchymal stem cells under the fetal bovine serum concentration gradient, Lab on a Chip, 7(2007) 1673-80.

[193] D. Jin, X. Ma, Y. Luo, S. Fang, Z. Xie, X. Li, et al., Application of a microfluidic-based perivascular tumor model for testing drug sensitivity in head and neck cancers and toxicity in endothelium, RSC Advances, 6(2016) 29598-607.

[194] E.W. Young, D.J. Beebe, Fundamentals of microfluidic cell culture in controlled microenvironments, Chemical Society Reviews, 39(2010) 1036-48.

[195] S.-F. Chang, C.A. Chang, D.-Y. Lee, P.-L. Lee, Y.-M. Yeh, C.-R. Yeh, et al., Tumor cell cycle arrest induced by shear stress: Roles of integrins and Smad, Proceedings of the National Academy of Sciences, 105(2008) 3927-32.

[196] L. Kim, Y.-C. Toh, J. Voldman, H. Yu, A practical guide to microfluidic perfusion culture of adherent mammalian cells, Lab on a Chip, 7(2007) 681-94.

[197] J.W. Song, W. Gu, N. Futai, K.A. Warner, J.E. Nor, S. Takayama, Computer-controlled microcirculatory support system for endothelial cell culture and shearing, Analytical chemistry, 77(2005) 3993-9.

[198] A. Zuchowska, E. Jastrzebska, K. Zukowski, M. Chudy, A. Dybko, Z. Brzozka, A549 and MRC-5 cell aggregation in a microfluidic Lab-on-a-chip system, Biomicrofluidics, 11(2017) 024110.

[199] L.J.Y. Ong, A.B. Islam, R. DasGupta, N.G. Iyer, H.L. Leo, Y.-C. Toh, A 3D printed microfluidic perfusion device for multicellular spheroid cultures, Biofabrication, 9(2017) 045005.

[200] Y.-s. Torisawa, B. Mosadegh, G.D. Luker, M. Morell, K.S. O'Shea, S. Takayama, Microfluidic hydrodynamic cellular patterning for systematic formation of co-culture spheroids, Integrative Biology, 1(2009) 649-54.

[201] Y. Sakai, K. Hattori, F. Yanagawa, S. Sugiura, T. Kanamori, K. Nakazawa, Detachably assembled microfluidic device for perfusion culture and post‐culture analysis of a spheroid array, Biotechnology journal, 9(2014) 971-9.

[202] M. Zanoni, F. Piccinini, C. Arienti, A. Zamagni, S. Santi, R. Polico, et al., 3D tumor spheroid models for in vitro therapeutic screening: a systematic approach to enhance the biological relevance of data obtained, Scientific reports, 6(2016).

[203] X. Cui, S. Dini, S. Dai, J. Bi, B. Binder, J. Green, et al., A mechanistic study on tumour spheroid formation in thermosensitive hydrogels: experiments and mathematical modelling, RSC Advances, 6(2016) 73282-91.

[204] M.J. Ware, K. Colbert, V. Keshishian, J. Ho, S.J. Corr, S.A. Curley, et al., Generation of homogenous three-dimensional pancreatic cancer cell spheroids using an improved hanging drop technique, Tissue Engineering Part C: Methods, 22(2016) 312-21.

[205] K.I. Au Ieong, C. Yang, C.T. Wong, A.C. Shui, T.T. Wu, T.-H. Chen, et al., Investigation of Drug Cocktail Effects on Cancer Cell-Spheroids Using a Microfluidic Drug-Screening Assay, Micromachines, 8(2017) 167.

[206] A. St-Georges-Robillard, M. Massea, J. Kendall-Dupontb, M. Struplera, B. Patraa, M. Jermynd, et al., Spectroscopic imaging system for high-throughput viability assessment of ovarian spheroids or microdissected tumor tissues (MDTs) in a microfluidic chip. dans, Photonic Therapeutics and Diagnostics XII, 9689(2016) 96894E1-5.

[207] P.M. Misun, J. Rothe, Y.R. Schmid, A. Hierlemann, O. Frey, Multi-analyte biosensor interface for real-time monitoring of 3D microtissue spheroids in hanging-drop networks, Microsystems & Nanoengineering, 2(2016) 16022.

[208] Y.R. Schmid, S.C. Bürgel, P.M. Misun, A. Hierlemann, O. Frey, Electrical Impedance Spectroscopy for Microtissue Spheroid Analysis in Hanging-Drop Networks, ACS Sensors, 1(2016) 1028-35.

[209] F. Alexander, S. Eggert, J. Wiest, A novel lab-on-a-chip platform for spheroid metabolism monitoring, Cytotechnology, (2017) 1-12.

[210] C.M.B. Ho, S.H. Ng, K.H.H. Li, Y.-J. Yoon, 3D printed microfluidics for biological applications, Lab on a Chip, 15(2015) 3627-37.

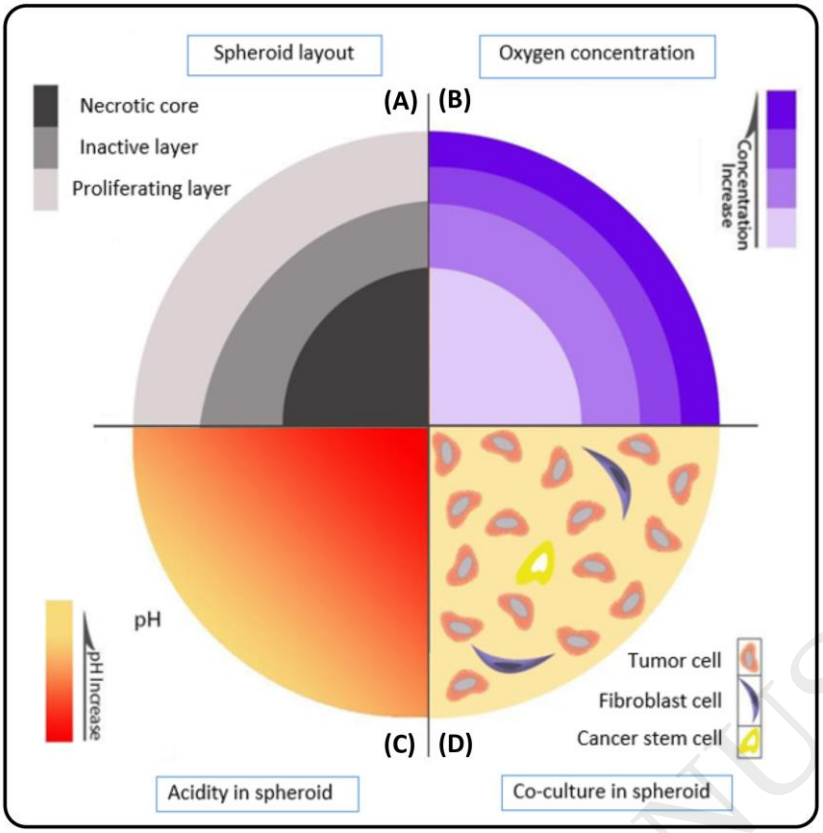

Figure 1. Tumor spheroid characteristics. (A) The three cell layers, distinguished by the rate of proliferation; (B) oxygen concentration gradient in tumor spheroid; (C) the pH gradient shows the existence of an acidic environment in the core as a result of anaerobic activities; (D) shows cells and the surrounding ECM in a co-cultured tumor spheroid.

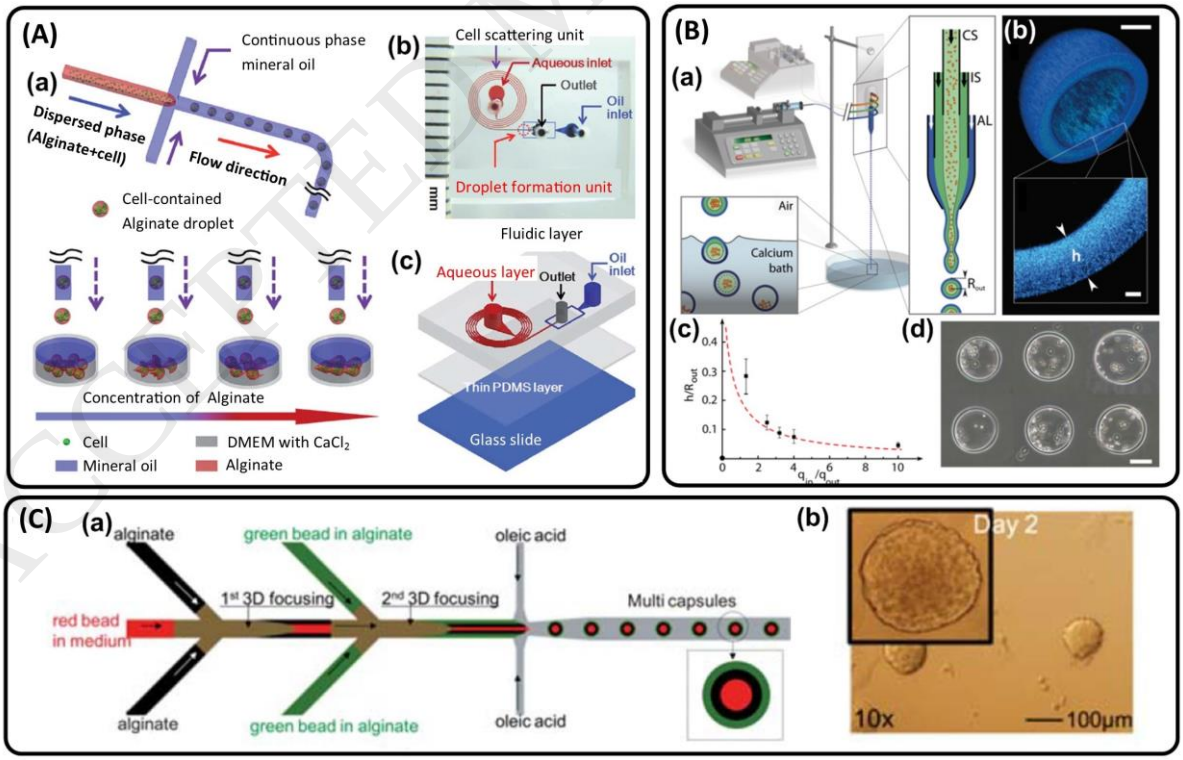

Figure 2. Emulsion-based techniques for spheroid formation. (A) (a) Schematic illustration of a single-emulsion (Gel/O) droplet generator for the formation of uniform water droplets containing different concentrations of alginate and cells dispersed in mineral oil in a

flow-focusing microfluidic device; (b and c) an overview and composition of the actual microfluidic device. Reproduced with permission from [100]. (B) (a) Schematic overview of a microfluidic device for multicellular spheroid production. The system is composed of an external fluidic injection system, coextrusion microdevice, and off-chip gelation bath; (b) Confocal image of an alginate capsule stained with high-molecular-weight fluorescent dextran; (c) Plot of the capsule aspect ratio as a function of the flow rate; and (d) Phase-contrast pictures of individual capsules encapsulating cells. Reproduced with permission from [101]. (C) (a) Schematic overview of a three-dimensional microfluidic system for generation of core-shell microcapsules for efficient formation of cell spheroids; (b) Representative phase-contrast micrographs of individual capsules encapsulating cells. Reproduced with permission from [98].

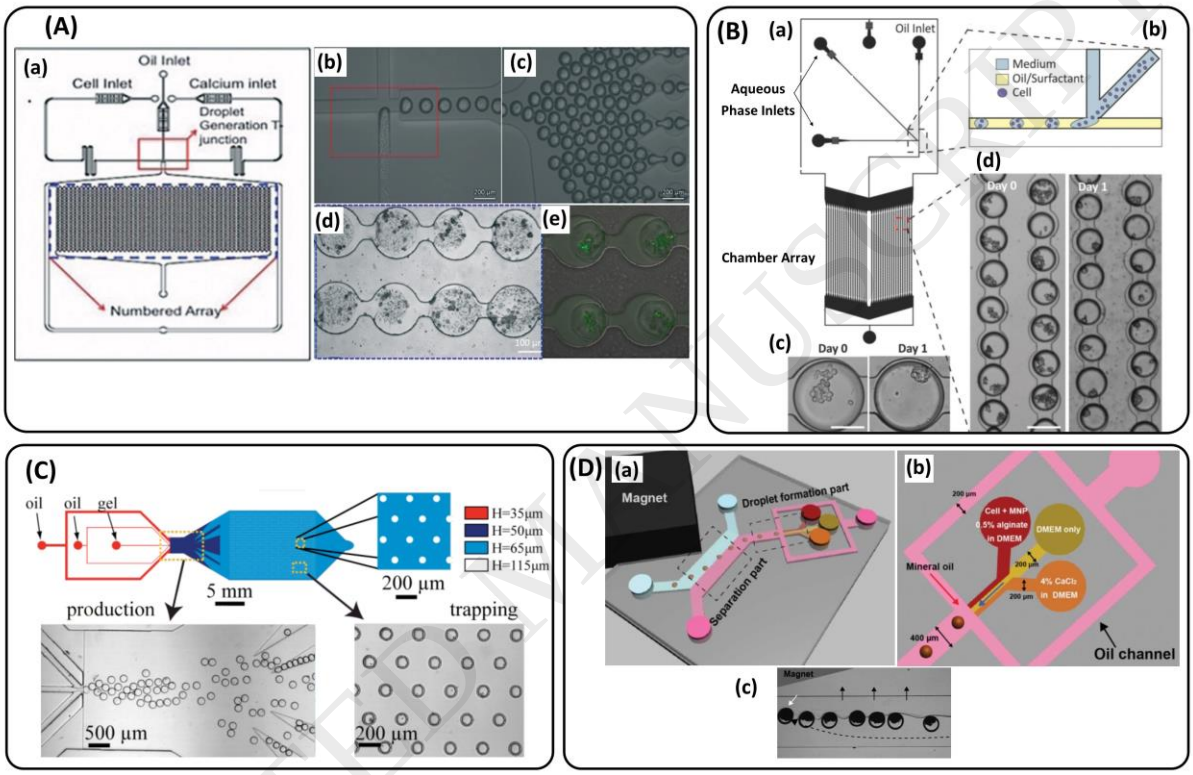

Figure 3. (A) Single-emulsion (Gel/O) droplet generation chip for spheroid generation having sinusoidal anchoring array for (a) single cell type encapsulation ; (b and c) T-junction for droplet formation and droplets entering the array before gelation; (d) Gelled cell-laden alginate spheroids; (e) Live cells stained with Calcein-AM. Reproduced with permission from [36]). (B) Single-emulsion (CS/O) spheroid formation device containing sinusoidal anchoring arrays. (a) Device overview showing the inlets and the anchoring array having 2000 droplet sites; (b) Droplet formation and cell encapsulation. (c and d) Brightfield images of cells encapsulated within droplets and trapped within the anchoring array (Reproduced with permission from [103]). (C) Single-emulsion (Gel/O) device using microwells to anchor cell-dispensed hydrogel droplets. (a) A schematic showing the oil and the hydrogel inlets and 2200 anchoring sites within the blue area; (b) Droplet production stage and the V-shaped trails for distributing the droplets over the anchoring sites. Reproduced with permission from [104]. (D) Another single-emulsion (Gel/O) chip producing droplets having magnetic particles on which magnetic force is exerted to deviate their pathway from the oil flow (pink) to the culture medium flow (blue). (a) Schematic depicting the overall view of the microfluidic chip; (b) The droplet generation section has four inlets: one dedicated to mineral oil and the others for $CaCl_2$, culture medium and cell dispensed alginate hydrogel solved in culture medium; (c) A microscopic image of the separation channel. The magnet attracts the gelled droplets containing cells and magnetic nanoparticles to make them enter the culture medium from the

oil. The broken line indicates the path line of a droplet. Reproduced with permission from [105].

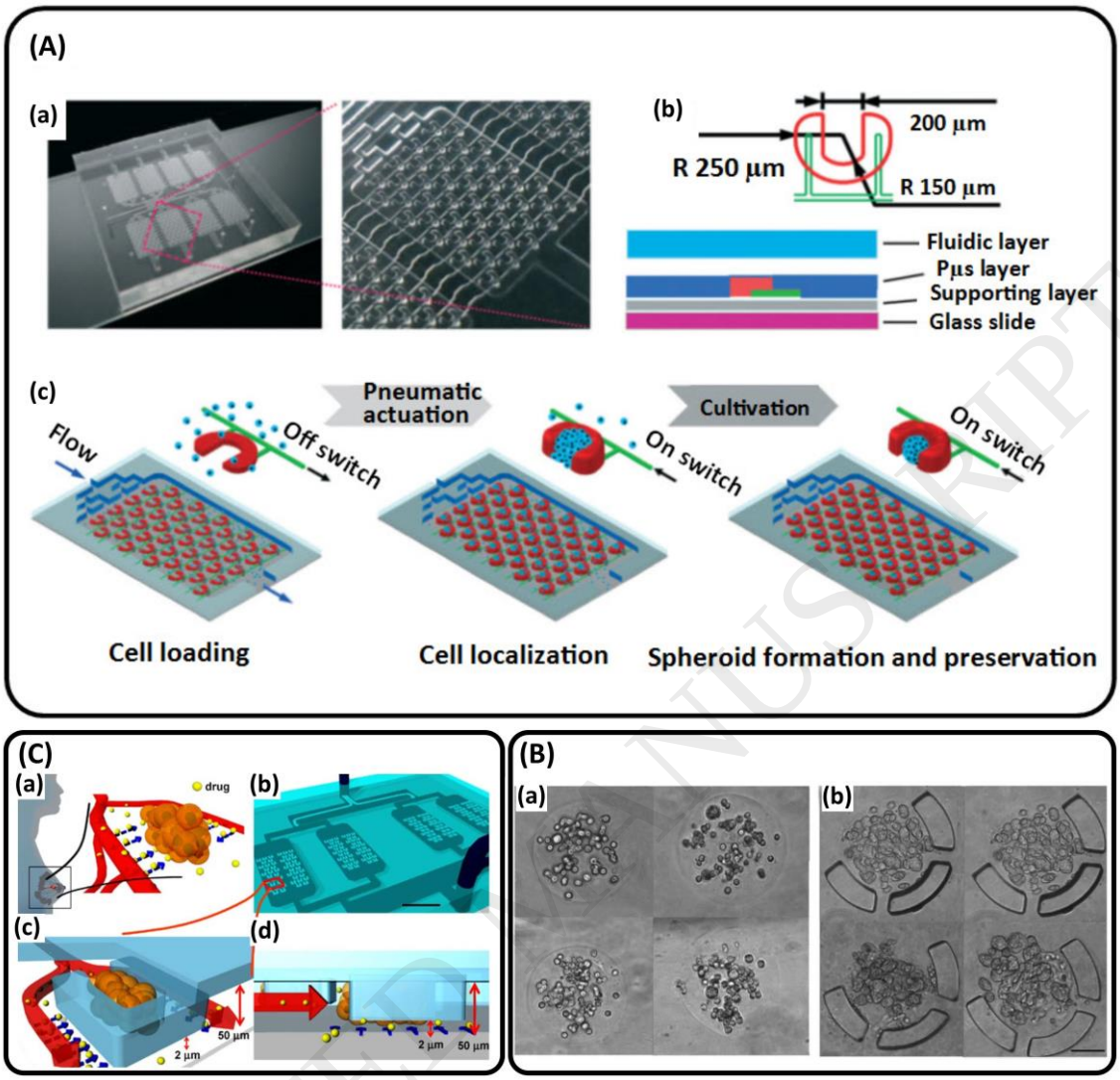

Figure 4. U-shaped microstructures in µSFCs: (A) A pneumatically actuated µSFC containing U-shaped microstructure arrays. It contains eight chambers for high-throughput cell trapping and spheroid formation. (a) The two images depict the microchip fabricated out of PDMS; (b) Top and sectional view of one of the U-shaped microstructures comprised of three layers; (c) Schematic diagrams of high-throughput cell loading and localization within the chip. Reproduced with permission from [128]. (B) Permanent U-shaped microstructures. (a) The configuration of the alginate encapsulated beads instantly after droplet formation, in a Petri dish; (b) This figure depicts the droplets four days after being trapped in the microsieve structures for spheroid formation. The gaps between the microsieves enable proper diffusional nutrient and gas exchange. Reproduced with permission from [18]. (C) A µSFC containing permanent U-shaped microstructures. (a) A representation of an in-vivo tumor provided by drug molecules from blood vessels; (b) The microchip constructed by PDMS/glass slide; (c and d) the flow of culture medium towards the microstructure pushes the cells inside. Drug, nutrient and waste molecules are perfused to the trapped cells with the flow through the 2 µm gap. Reproduced with permission from [121].

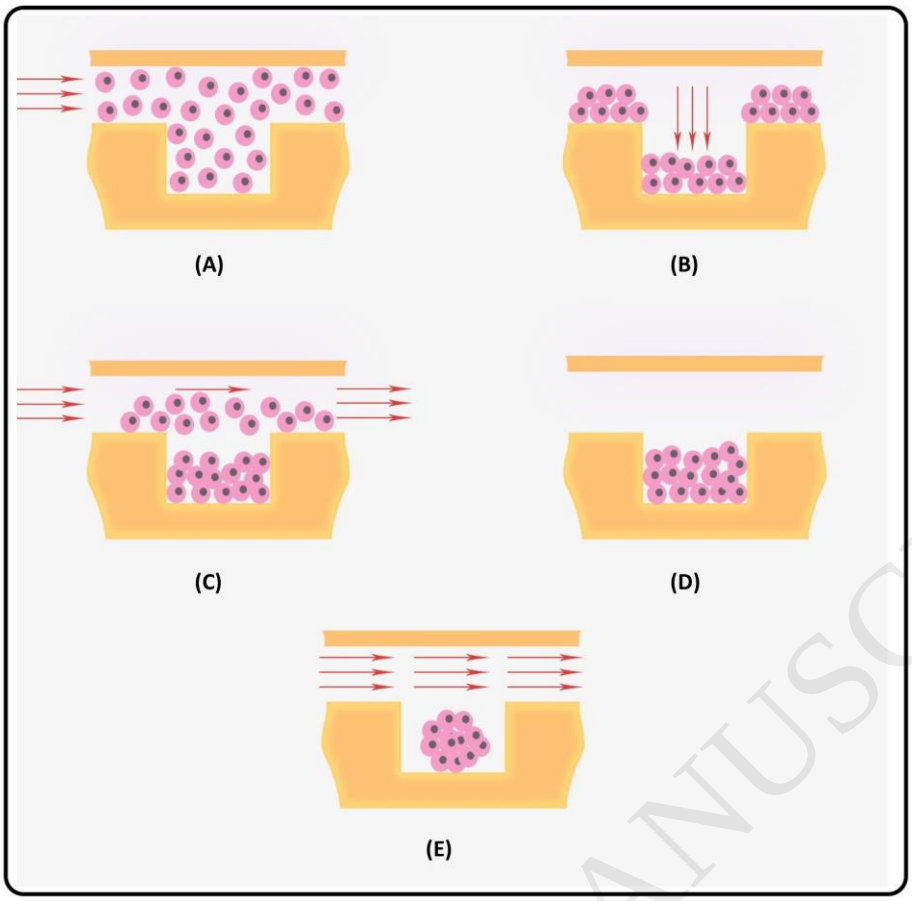

Figure 5. Spheroid formation process in a microwell-based µSFC: (A) Introduction of a cell suspension to the chip inlet. The cell suspension fills all the microchannels and microwells rapidly due to the capillary effect; (B) Cells start depositing on the bottom of the microchannels and microwells; (C) Pure culture medium flows through the chip to rinse the excess cells without disturbing the cells lying on the microwell bottom; (D) Cell secretions and signaling lead to establishment of cell-cell interactions on the non-adherent microwell bottom; (E) Driving spheroid formation under a perfusing flow of culture medium.

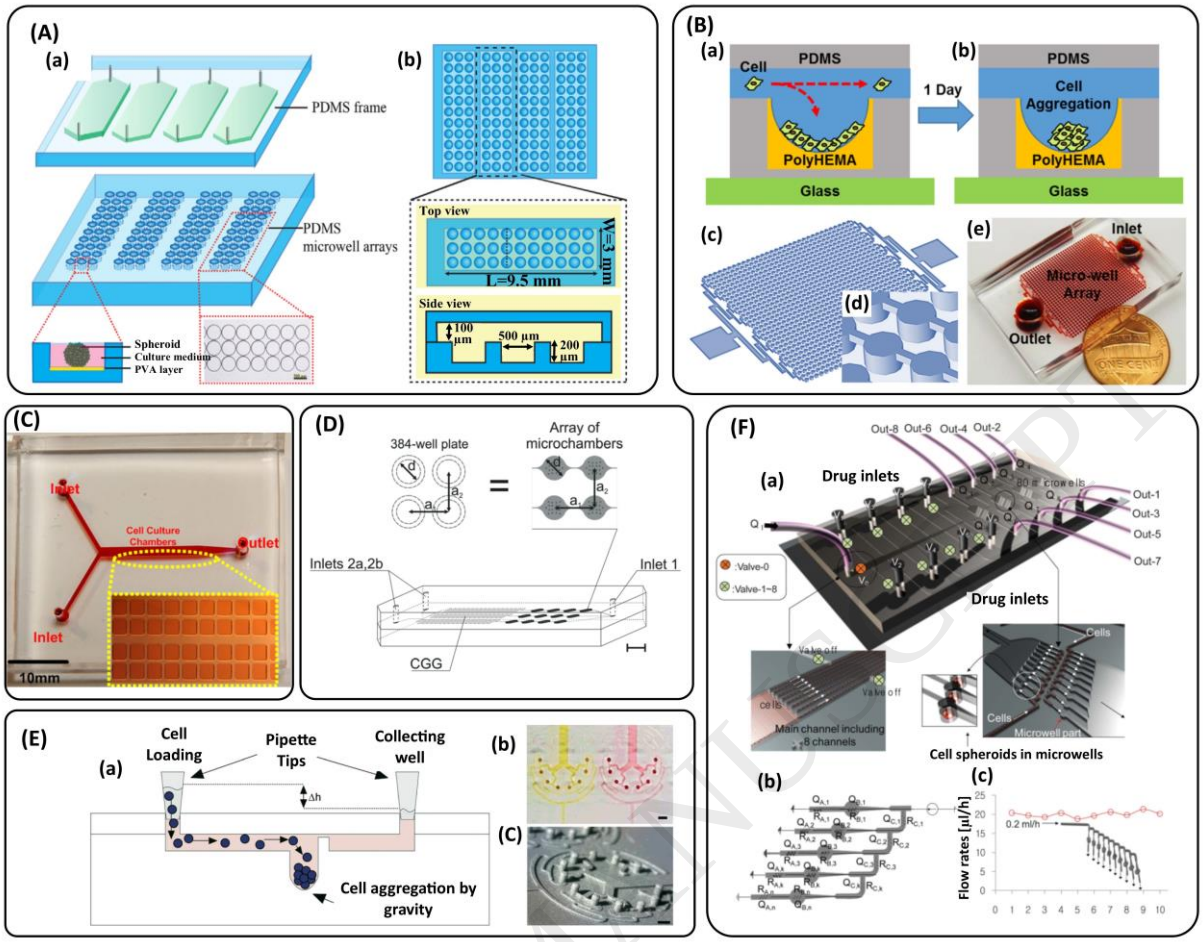

Figure 6. Parts A to D depict microwell-based µSFCs in which each microchannel feeds several spheroids. In the parts E and F each main microchannel branches into several microchannels which individually feed each microwell. (A) A graphic demonstration of a microchip for MTS formation and drug screening. (a) Each microchannel feeds a 3×11 configuration of microwells. The formation of a cell spheroid on a microwell displayed at the bottom left, and a micrograph of the microwell-array of the chip is shown at the bottom right; (b) Top and side visions of the microchip. Reproduced with permission from [134]. (B) A microwell-based µSFC for evaluating the efficacy of Photo Dynamic Therapy on tumor spheroids. (a) Graphical representation of cells trapping in a microwell; (b) Schematic of cell aggregation after 1 day; (c and d) The structure of the 3D microfluidic chip; (e) The fabricated chip that has 1024 microwells within a main area of 2 cm by 2 cm. Reproduced with permission from [13]. (C) Photographs of a two-layered µSFC, and the magnified view of the square spheroid culture microwells in the inset. Reproduced with permission from [96]. (D) A µSFC integrated with a CGG to facilitate high-throughput drug tests. Each drug is delivered to three microchambers in series, each containing 14 microwells. The distance between microchambers was designed such that the µSFC is compatible with conventional plate readers. Reproduced with permission from [6]. (E) A microwell-based µSFC having (a) Cells are trapped within each microwell due to the difference between the inlet and outlet microchannel heights; (b) Top-view of two microchannels filling with color food dyes (yellow and red). The length of the microchannels delivering cell suspension to each microwell is equal to facilitate uniform-sized spheroid formation; (c) The microchip's mold made of epoxy. Reproduced with permission from [39]. (F) A microwell-based µSFC designed using the hydraulic-electric analogy to facilitate spheroid culture of the same cell numbers in all the microwells. (a) It contains one inlet for cell seeding, eight inlets for drug perfusion and eight outlets; (b) Plane representation of the microchannel network in which the

flow rates are adjusted by the hydrodynamic resistance of the microchannels; (c) The uniform flow rates in each microchannel estimated by hydrodynamic simulation. Reproduced with permission from [88].

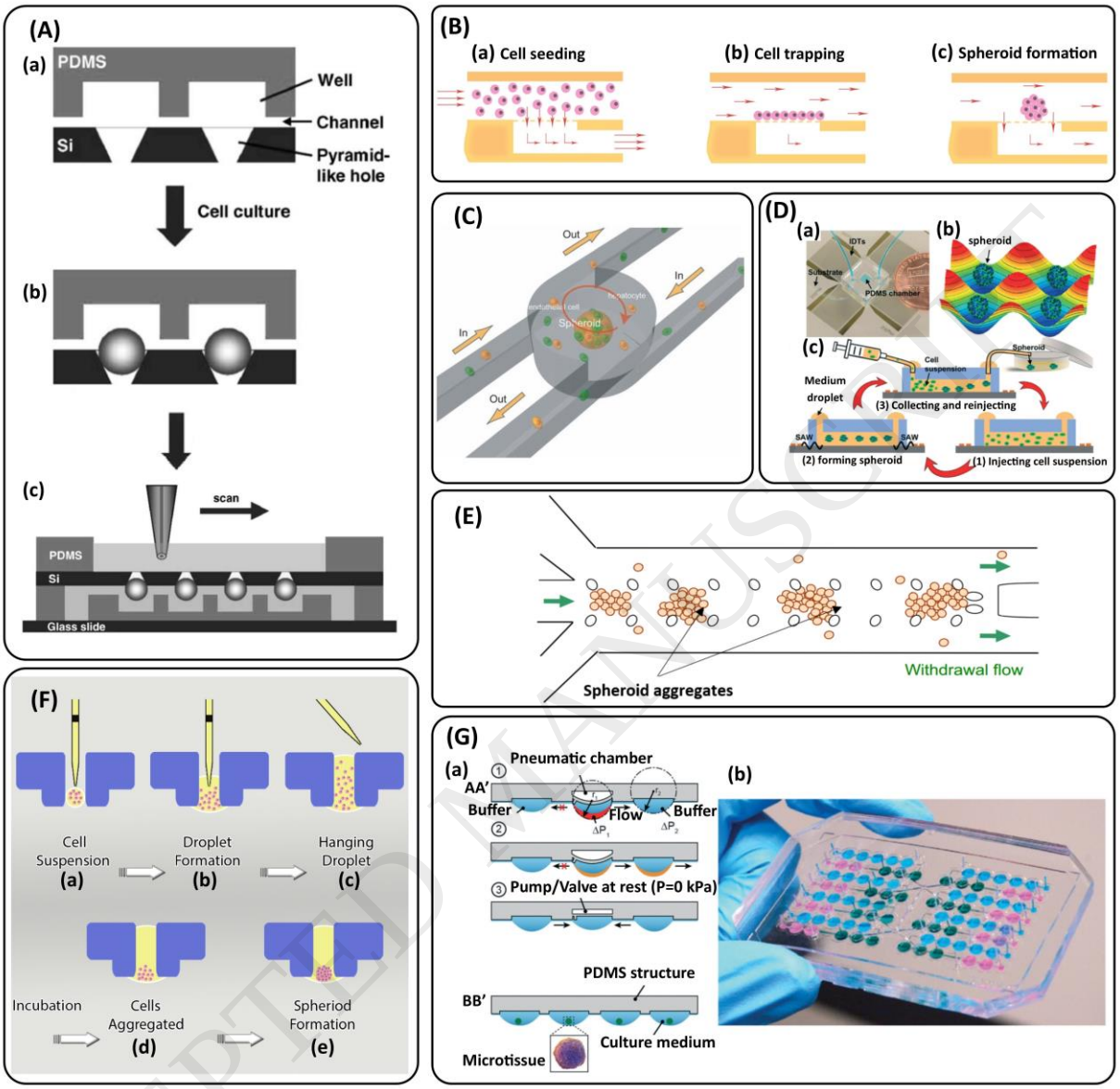

Figure 7. Other types of µSFCs: (A) A µSFC compatible with SECM due to silicon pyramid-like holes. (a) The cross-section of the microchip is depicted and its layers are shown; (b) The figure shows the microchip after spheroids have been formed in the structures resembling HDs; (c) The SECM measurement was done on the microchip while it was inverted on a glass slide to avoid spilling of the measurement liquid. Reproduced with permission from [151]. (B) Cell trapping behind a porous membrane for spheroid formation, facilitated by the flow of the cell suspension through the membrane. The spheroid formation is carried out by: (a) cell seeding, (b) cell trapping behind the porous membrane and (c) cell aggregation. (C) Microrotational flow in a microchamber having two inlets and outlets embedded in a three-layered µSFC. The inlet and outlet channels are tangential to the cylinder in the middle layer and the upper layer, respectively, to promote rotational flow. Reproduced with permission from [152]. (D) Spheroid formation by the aid of 3D acoustic tweezers. (a) The overall view of the microchip is shown; (b) Diagram of Gor'kov potential field inside the cavity. The balance among the acoustic radiation force, microstreaming drag force, gravity and buoyant force aggregated the Cells; (c) First, the cell suspension is injected. Then,

spheroids are formed in the microchannel where the potential field exists; the generated spheroids are then placed in a Petri dish. Reproduced with permission from [10]. (E) Cells are entered through the central inlet channel and trapped in the central chamber to form spheroids. The chamber is separated from the surrounding flow, which comes through the side inlets, by micropillars which are located close to each other. Reproduced with permission from [153]. (F) HD spheroid formation in an HD plate: (a) introduction of the cell suspension within the holes; (b) formation of the droplet by the capillary forces, (c) creation of an HD, (d) cell aggregation, (e) spheroid formation after one day. Redrawn after [54]. (G) an HD based µSFC. (a) The figure depicts (1) the pneumatic chamber is pressurized to create a flow from the central HD to the right HD (2). (3) The left valve, which prevented backflow, is now open while the pneumatic chamber is unpressurized. Figure (4) shows the spheroids in the HDs; (b) an image of the HD based µSFC which is colored by food dyes. Reproduced with permission from [154];

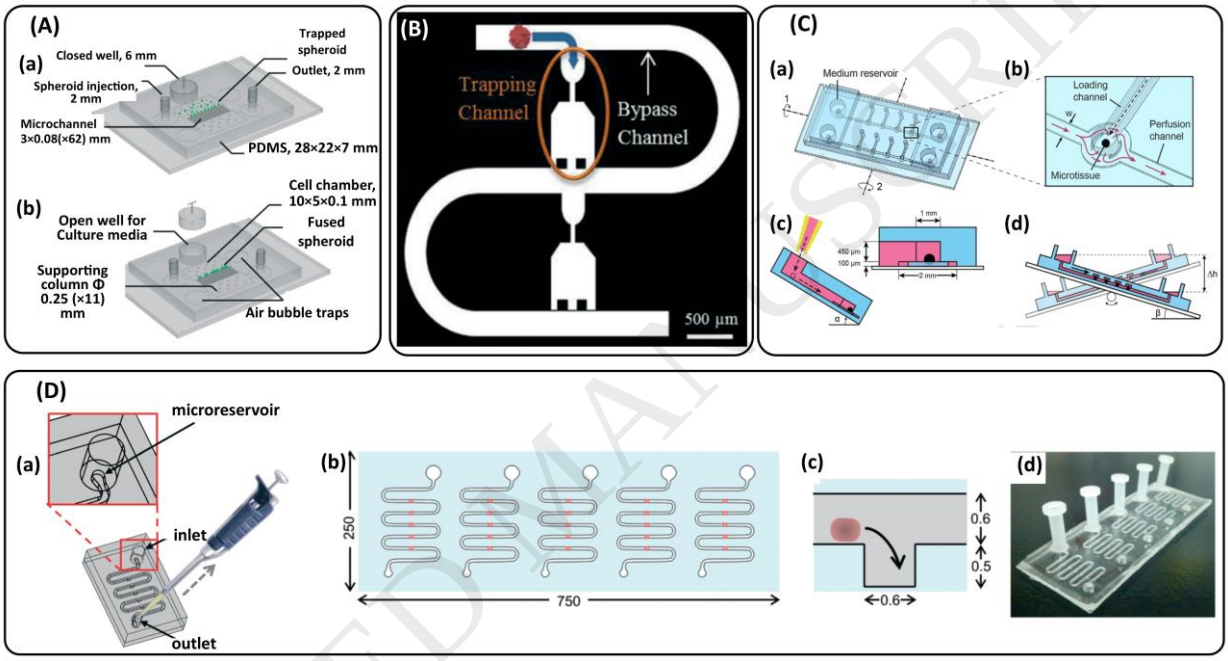

Figure 8. The figure depicts various µSCCs. (A) A µSCC for culturing olfactory ensheathing cell spheroids. (a) This device consists of two inlets: one large well (6 mm) for culture medium and a smaller one (2 mm) for spheroid injection. Parallel microchannels, 80 µm in width for spheroid trapping, are embedded within the device through which the culture medium passes and feeds the spheroids; (b) the device also integrates lateral chambers for trapping unwanted air bubbles entering the device. Reproduced with permission from [87]. (B) The microchannels are designed using the hydraulic-electric analogy in which the trapping channel has less flow resistance than the bypass channel before spheroid trapping. Reproduced with permission from [8]. (C) A hydrostatic pressure-driven µSCC containing two units each having one perfusion and four loading microchannels. (a) Medium reservoirs are situated at both ends of each perfusion microchannel; (b) the spheroid culture chamber is placed at the intersection of the loading and the perfusion microchannel; (c) to load spheroids, the device is slanted with respect to axis No. 1 in figure (a); (d) After spheroid loading into the chambers, flow is created by periodic tilting of the device around axis No. 2 to obtain hydrostatic pressure difference between the inlet and outlet. Reproduced with permission from [89]. (D) A µSCC consisting of five parallel sinuous microchannels each of which contains five microwells for sedimentation trapping of the loaded microtissues or spheroids. (a) Loading microtissues or spheroids into the chip by a micropipette; (b) The microchip with five independent microchannels each has five equally-spaced microwell traps (red); (c) side

view of the microtissue in the microchannel which is reaching the microwell trap; (d) the microchip made of PDMS with five inlet reservoirs. Reproduced with permission from [139].

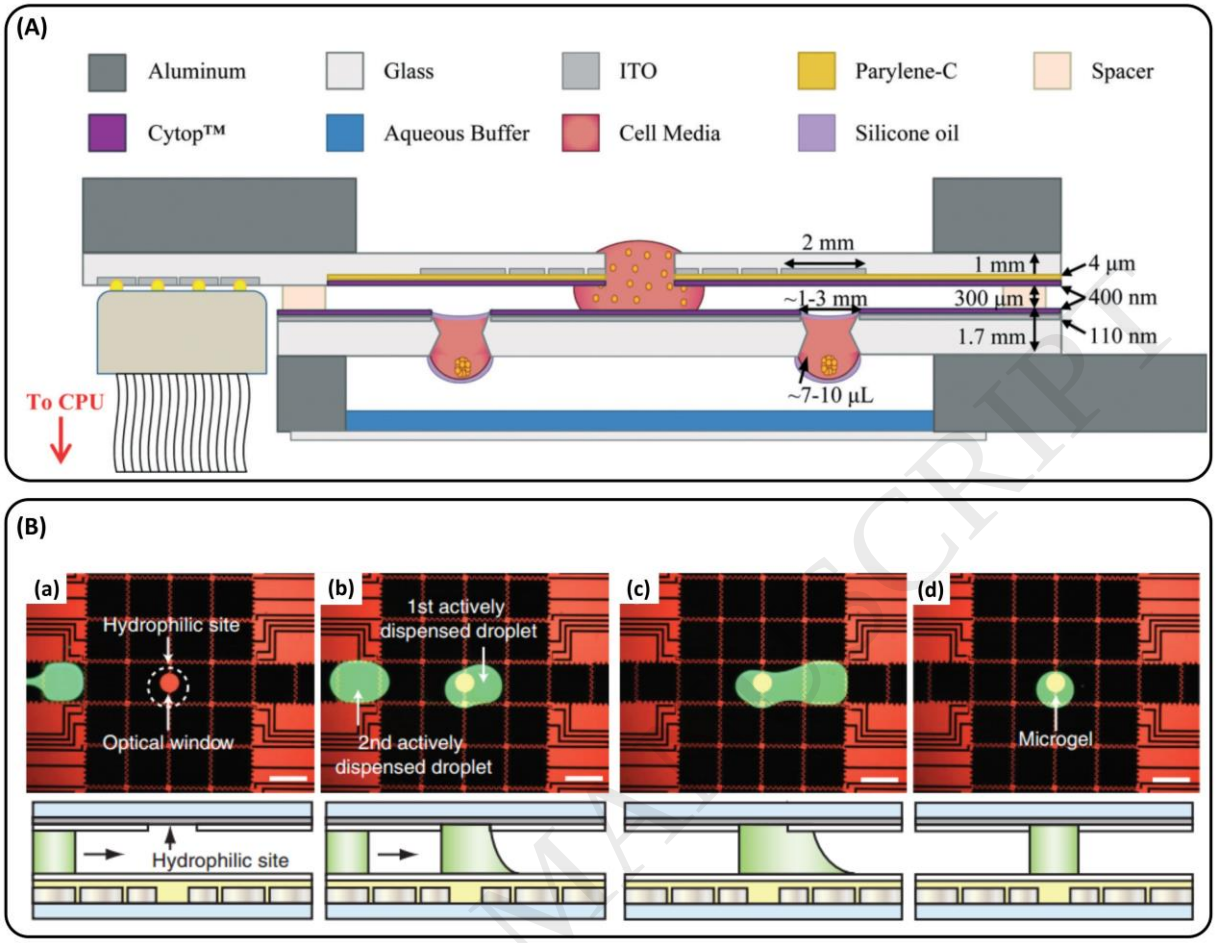

Figure 9. Digital microfluidic chips for spheroid formation. (A) An HD-based digital µSFC. As shown in the figure, the platform design is complex and needs several materials such as Aluminum, Parylene-C, silicon oil, etc. as well as high resolution in fabrication (400 and 110 nm layers). A cell suspension is first introduced to the device inlet. Then, droplets are guided to the sites where the holes exist by the aid of capillary forces in order to form HDs and spheroids consequently. The humidified environment is provided by a buffer to prevent droplet evaporation for the long-term experiment. Reproduced with permission from [173]. (B) The process of droplet manipulation and anchoring in a digital microfluidic chip: (a) introducing the first droplet to the chip and guiding it to the hydrophilic site; (b) anchoring of the first droplet and introducing the second droplet to the first droplet; (c) the droplet moves across the hydrophilic site to facilitate the formation of a droplet similar to the hydrophilic pattern; (d) cross-linking leads to forming a solid microgel. Reproduced with permission from [178].

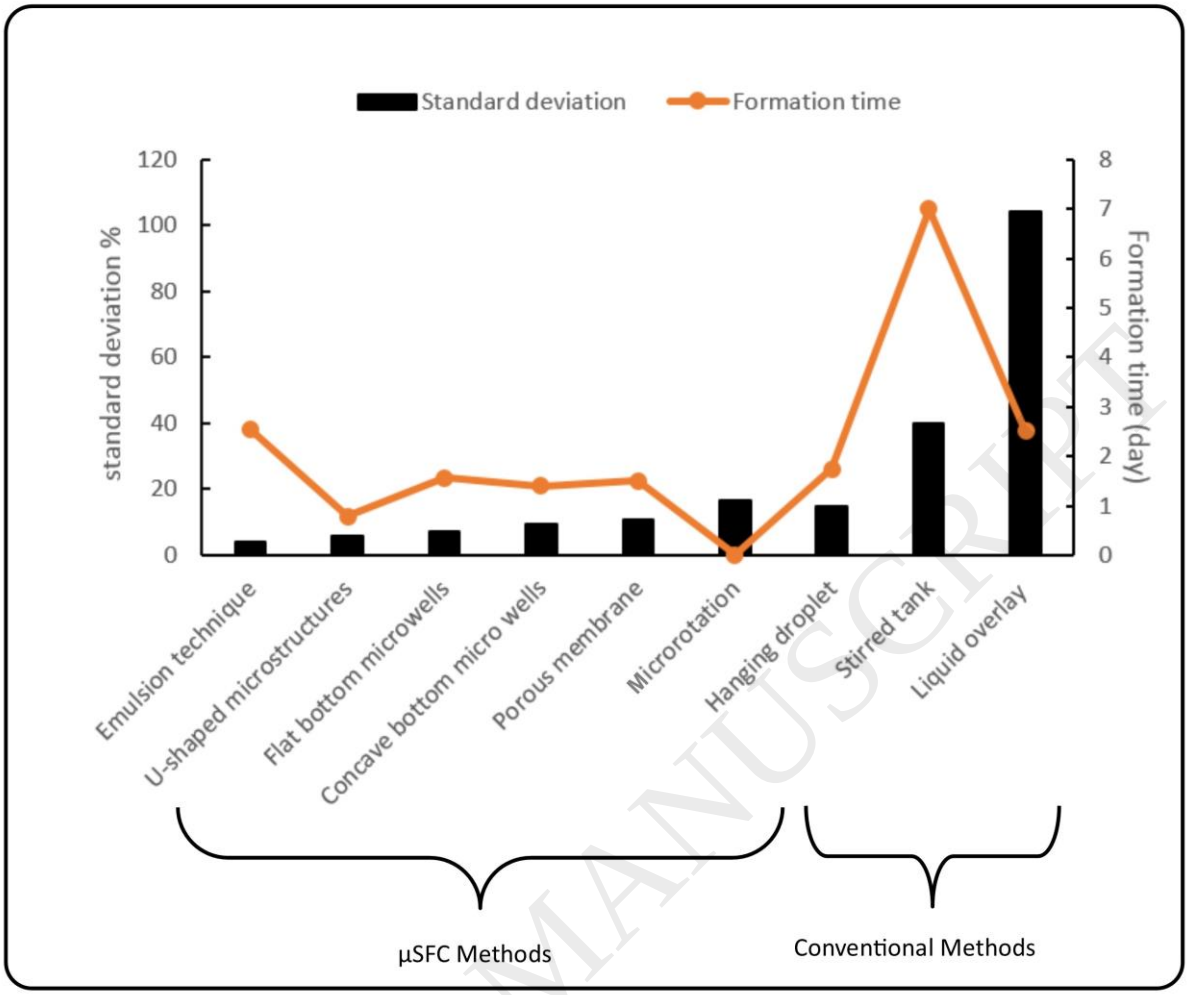

Figure 10. The figure shows spheroid diameter standard deviation (the black columns) and formation time (the orange line) collected from a myriad of previous studies. The data belong to microfluidic and conventional methods for spheroid formation, displaying microfluidics' superior advantages in forming spheroids with a shorter time and also size uniformity. The SD extends from 4% for the emulsion technique to 16.6% for the microrotational flow µSFC. The formation time also differs significantly from the stirred tank method and µSFCs.

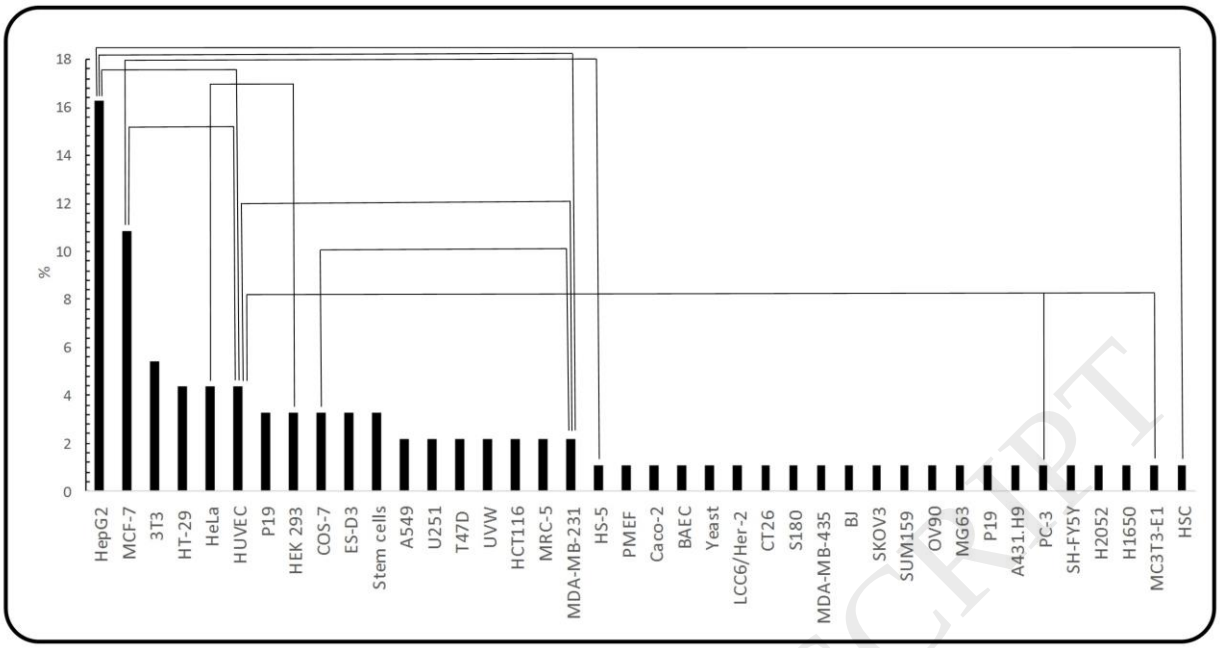

Figure 11: The figure depicts the various cell lines used for spheroid formation and co-culture assays on µSFCs and µSCCs. The bars show the percentage of the µSFCs or µSCCs in which these cell lines have used for spheroid formation and culture. For instance, the HepG2 cell has been used in almost 16.5% of the works found in the literature. To show the co-culture assays, the cell lines used have been attached together with the black lines. For example, in one work, the MCF-7 and the MDA-MB-231 cell lines are co-cultured.

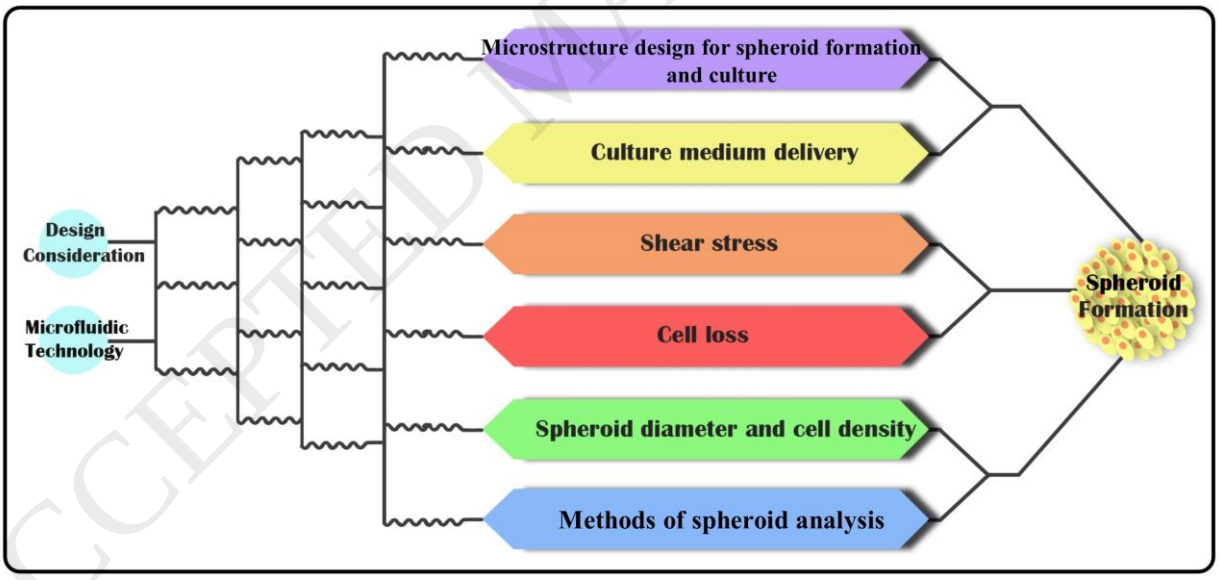

Figure 12. The design considerations which need to be considered for spheroid formation and culture in microfluidic chips.

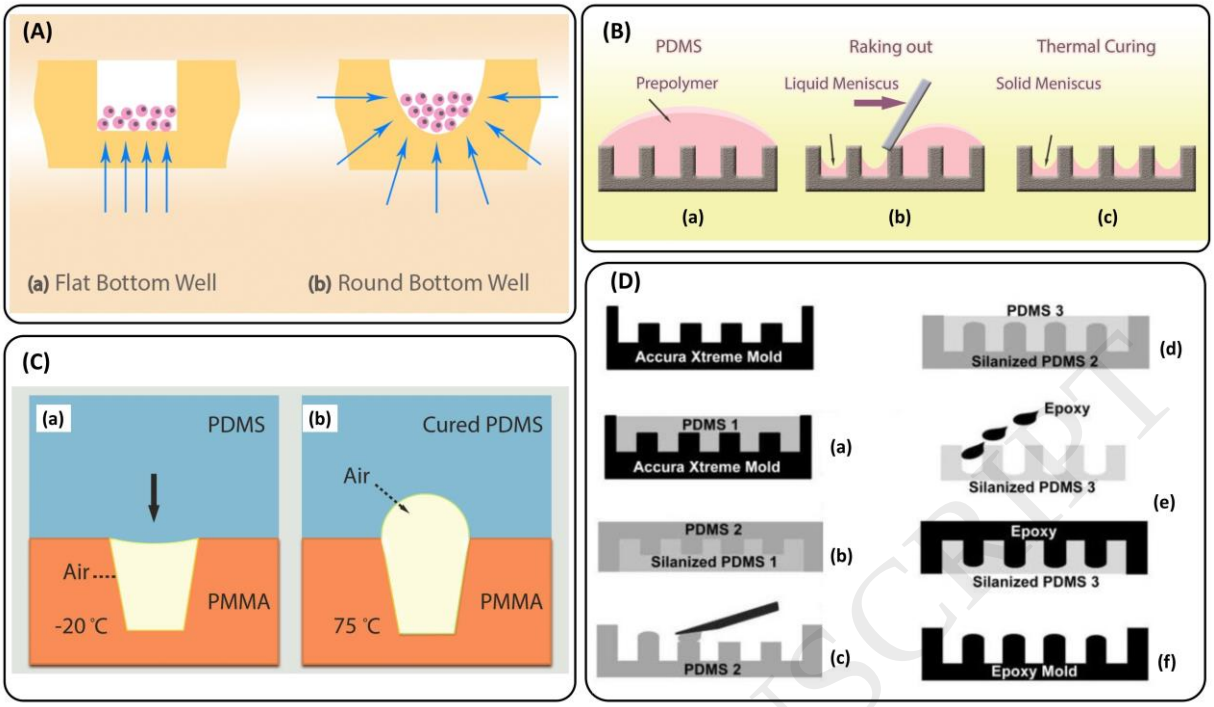

Figure 13. (A) Illustration of the microforces acting on cells in a (a) flat-bottomed and (b) concave-bottomed microwell. Figures B to D depict fabrication methods to generate concave-bottomed microwells for spheroid formation: (B) creating concave-bottomed microwells using PDMS prepolymer by: (a) pouring the PDMS prepolymer on the microwells; (b) raking out the liquid meniscus and (c) thermal curing for PDMS solidification. Redrawn after [40]. (C) Using air expansion to induce concave shape on PDMS slab: (a) air is trapped in the microwell due to the high viscosity of cold PDMS; (b) during baking of PDMS, the air expands and pushes the PDMS upward. After baking, the PDMS slab is peeled off and used. Redrawn after [125]. (D) This method utilized silanization treatment to enable multi-casting of PDMS. All PDMS curing took place at 60˚C for 2h. (a) Mold is filled with PDMS and cured. (b) After silanization a second PDMS is produced and cured. (c) A little drop of PDMS is added on every well to round it and cured. (d) After silanization a 3rd PDMS cast is produced and cured. (e) After silanization the PDMS mold is filled with the epoxy (Weildling C) and cured at 40˚C for 24h. (f) Final epoxy mold with round bottom wells. Reproduced with permission from [39].

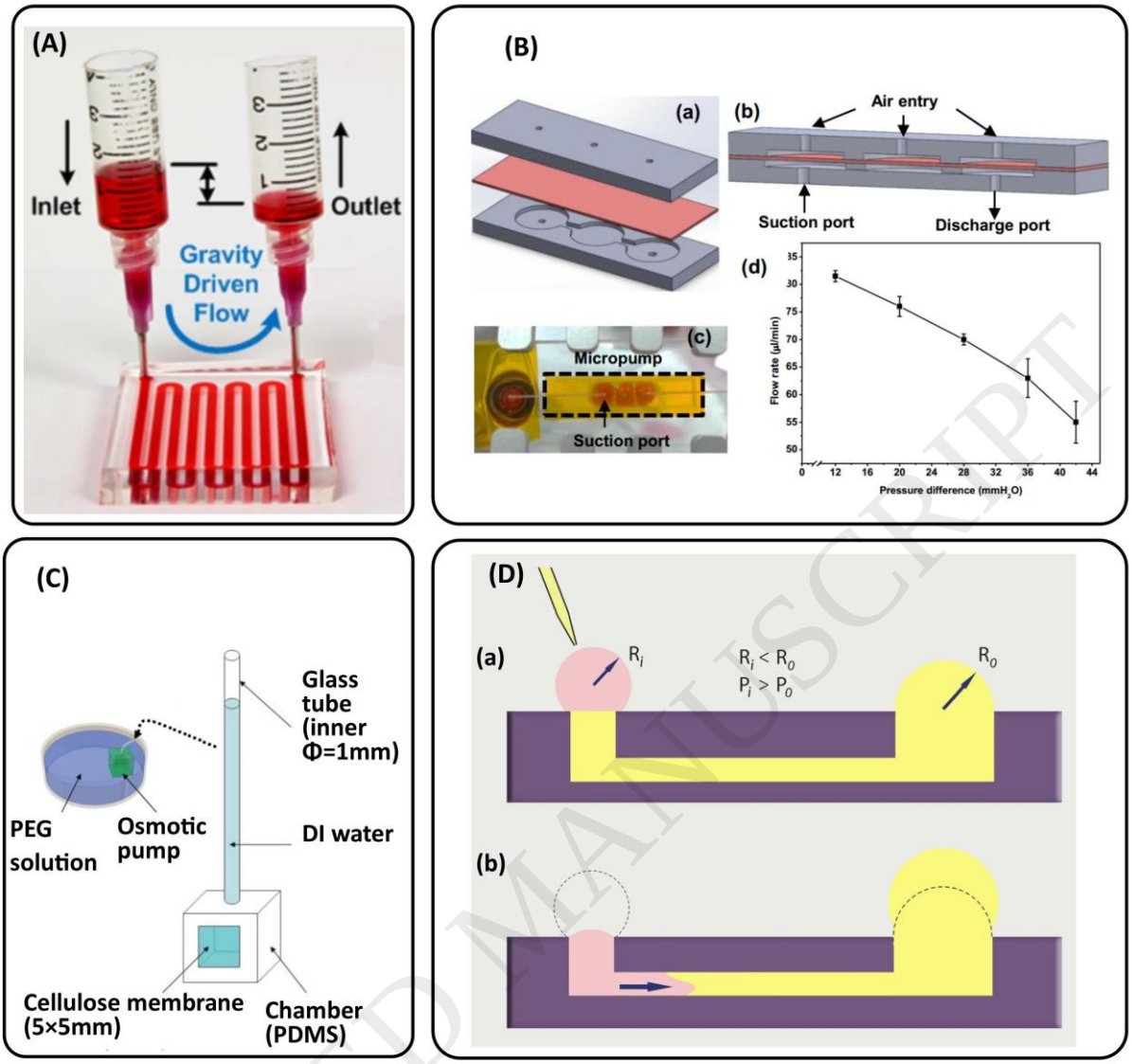

Figure 14. Various methods for flow pumping in microfluidic chips. (A) Hydrostatic pressure drives flow through a μSFC. Reproduced with permission from [7]. (B) Peristaltic pump designed by Mousavi et al. [188]. (a) Schematic view of the micropump consisting of three layers which are two PDMS layers in the top and bottom of the device in addition to a diaphragm layer (red). By inducing low pressures in the air entry, flow is promoted from the suction port to the central chamber. Conversely, when applying high pressure in the air entry, the liquid in the chamber flows towards the discharge port; (b) cross-sectional view, showing the air and the liquid ports; (c) overall view; (d) the diagram of the pumping flow rate vs. pressure difference of the micropump. Reproduced with permission from [188]. (C) Schematic view of an osmotic pump designed by Park et al. comprised of water in a glass tube, a PDMS chamber containing water and a cellulose membrane [192]. The chamber is placed in a dish containing poly (ethylene glycol) solution in order to encourage liquid flow from the cellulose membrane to the dish. Reproduced with permission from [192]. (D) Passive pumping is facilitated by: (a) putting droplets at the inlet and the outlet channels having different volumes; (b) promotion of flow through the device from the smaller droplet to the larger one as a result of Laplace pressure difference caused by liquid surface tension. Redrawn after [194].

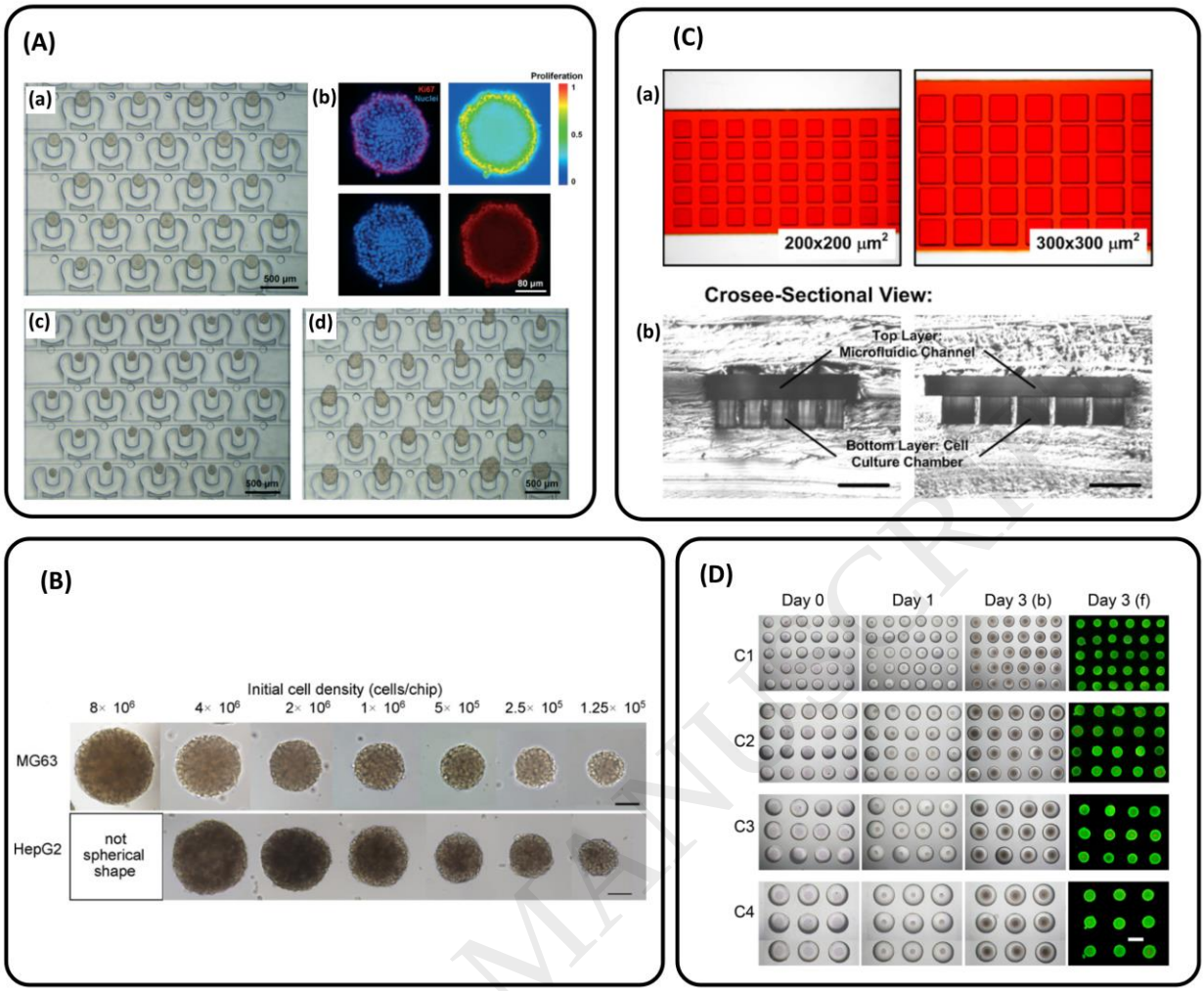

Figure 15. Different spheroid diameters formed by specific strategies. (A) Spheroid formation of cells having varied volumes in pneumatically-actuated microstructures. (a) Human glioma (U251) cell spheroids cultured for 10 days; (b) Fluorescence photography from Ki67 (red) and nuclear staining (blue) of U251 tumor spheroids after 10 days of culturing. The top right image indicates cell proliferation using fluorescence imaging of Ki67 in a spheroid cultured for 10 days in the μSFC; (c) human breast adenocarcinoma (MCF-7) cell spheroids after 10 days of culturing; (d) human hepatocellular liver carcinoma (HepG2) cell spheroids after 5 days of culturing. These cell lines have the same cell densities in the suspension which consequently results in distinct spheroid diameters for each cell line. Reproduced with permission from [128]. (B) Using various cell densities in the introduced cell suspension leads to differently-sized spheroids. Here, MG63 and HepG2 cell spheroids are shown after 5 days of culturing. Reproduced with permission from [185]. (C) Two sets of dimensions for square-sectioned microwells are shown. (a) Top view of the microwells having sides of 200 and 300 μm; (b) side cross-section view of the two sets of microwells. Reproduced with permission from [7]. (D) Various microwell diameters of C1, C2, C3 and C4 were used for spheroid formation. Images are taken on days 0, 1 and 3 after culturing from spheroids before and after live/dead cell staining. Reproduced with permission from [125].

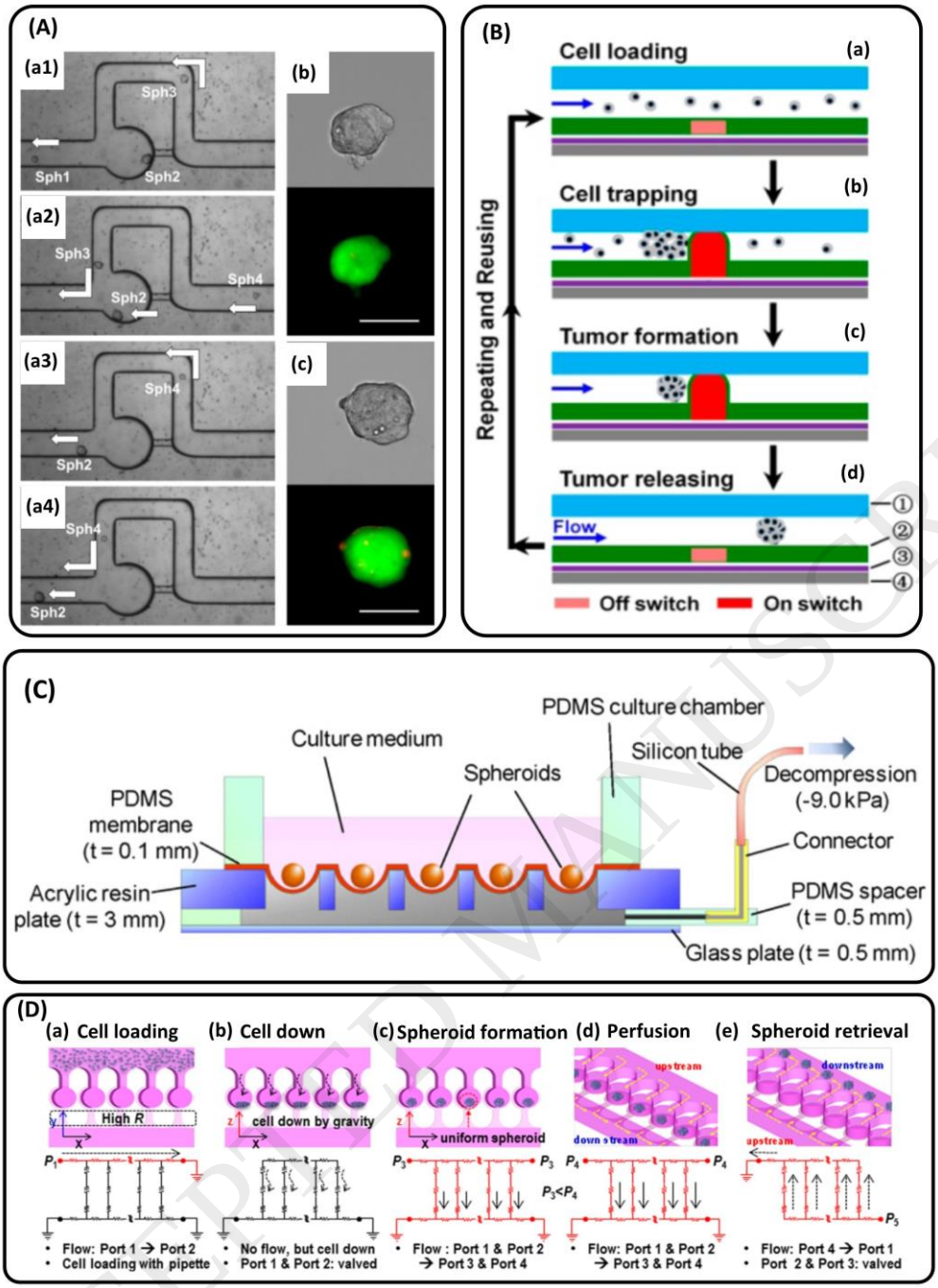

Figure 16. Summary of various methods used for spheroid retrieval in µSFCs. (A) (a1 to a4) The time-lapse image sequence of spheroid retrieval by reversing the flow direction; (b and c) brightfield and fluorescent images of the retrieved spheroids proved the success of the retrieval process. Reproduced with permission from [149]. (B) Spheroid retrieval by pneumatic actuation of a PDMS membrane. (a) Cell loading to the microchip; (b) blocking the flow by pressurizing the PDMS membrane to trap cells; (c) spheroid formation; (d) releasing the pressure to free the spheroids for retrieval. Reproduced with permission from [120]. (C) Forming microwells using PDMS membrane by pneumatic actuation. The acrylic resin plate contains many holes and is placed above the air chamber in the bottom layer of the microchip. The air chamber is connected to a vacuum pump with a silicon tube to induce pressure difference across the membrane. Reproduced with permission from [185]. (D) The procedure for spheroid generation and retrieval in a µSFC. (a) Loading cells by a pipette; (b) orienting the device vertically for cell sedimentation; (c) spheroid formation; (d) hydrostatically-driven

perfusion flow; (e) spheroid retrieval by reversing the flow direction in the chip. Reproduced with permission from [16].

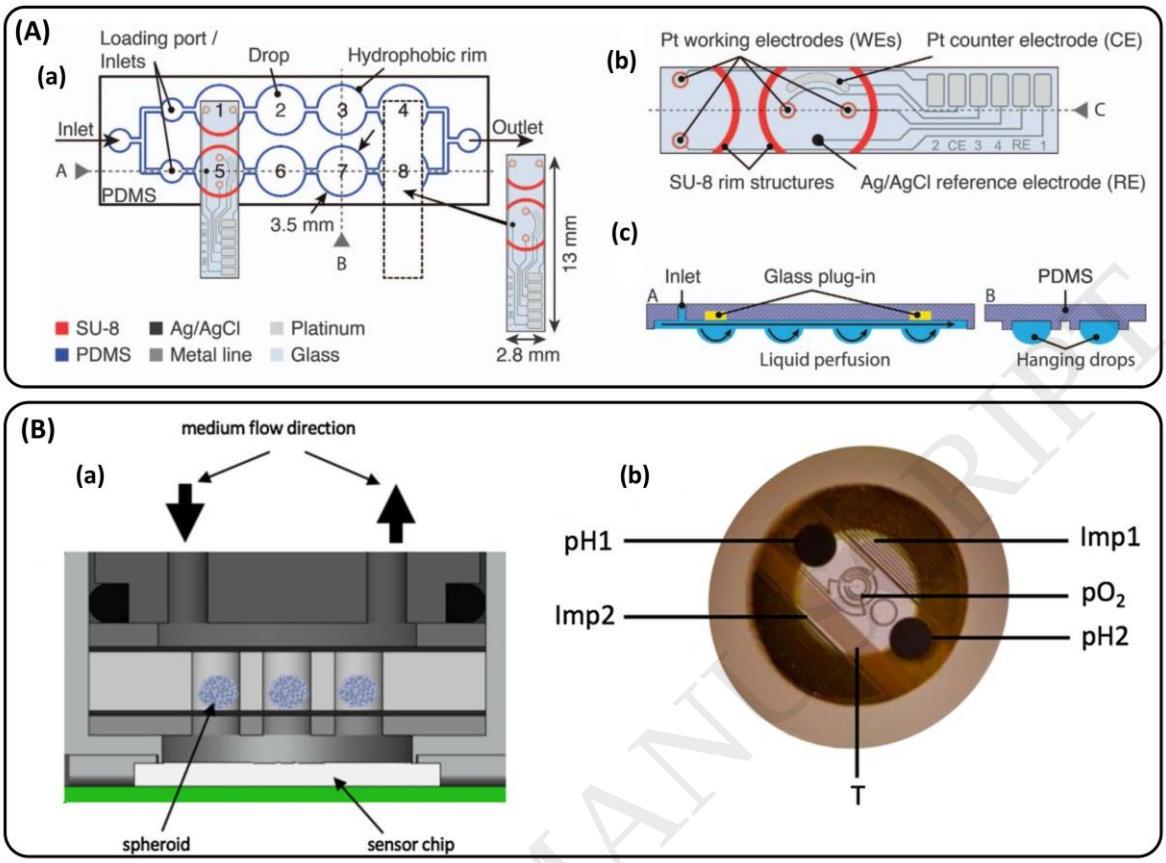

Figure 17: (A) An HD-based µSFC integrated with a biosensor for lactate and glucose measurements; (a) schematic view of the device having 8 HD sites of 3.5 mm diameter and the orientation of the biosensor on the chip; (b) the electrode-based biosensor is displayed. The sensor consists of four working platinum electrodes, one platinum counter electrode and an Ag/AgCl reference electrode; (c) the cross-section views A and B clarify the flow in the microchannels and the yellow glass plug-ins on which the sensors are deposited. Reproduced with permission from [207]; (B) A cross-sectional view of the µSCC (a) and the sensor chip (b) designed by Alexander *et al.* [209]; (a) It consists of a fluidic channel in the top, three 1 mm diameter microwells containing the spheroids and a sensor microchip in the bottom of the porous membranes; (b) the sensor chip measures the pH of the microenvironment (pH1 and pH2 sensors), oxygen uptake rate by the cells (pO_2 amperometric sensor), temperature (T) and electrical impedance (Imp1 and Imp2) by the electrodes shown in the figure. Reproduced with permission from [209];

Author biographies

Khashayar Moshksayan was born on May 1993. He graduated from Mechanical Engineering at Shiraz University, Iran, in 2015 and now is a MSc student at Sharif University of Technology, Iran. His research interests include microfluidics, biofluid mechanics, lab-on-a-chip, organ-on-a-chip, microfabrication and computational fluid dynamics (CFD). He is skilful in numerical analysis and CFD modeling in Ansys software and programming in MATLAB. Khashayar is currently working on design and fabrication of a microfluidic chip for three dimensional culture of cancer cells.

Navid Kashaninejad received his BSc and MSc degrees in Mechanical Engineering, Energy Conversion. In 2013, he obtained his PhD from the Division of Thermal and Fluid Engineering, Nanyang Technological University (NTU), Singapore. His PhD studies mainly focused on design and fabrication of microfluidic devices. His research interests include: design, fabrication and numerical simulation of microfluidic platforms for biological applications, and tissue engineering and regenerative medicine (e.g., fabrication of biomimetic scaffolds). He is currently a Research Fellow at Queensland Micro- and Nanotechnology Centre (QMNC), Griffith University, Australia

Majid Ebrahimi Warkiani is a Senior Lecturer in the School of Biomedical Engineering, University Technology Sydney (UTS), Sydney, Australia. He received his Ph.D. in Mechanical Engineering from Nanyang Technological University (NTU, Singapore), and undertook postdoctoral training at Massachusetts Institute of Technology (MIT, USA). He is also a member of Institute for Biomedical Materials & Devices (IBMD) and Center for Health Technologies (CHT) at UTS, a visiting scientist at the Garvan Institute for Biomedical Research as well as Translational Cancer Research Network (TCRN).

John G. Lock obtained his BSc (Honours 1st class) in Biochemistry and Cell Biology and his PhD in Cell Biology and from the University of Queensland, Australia. From 2006 to 2010, he was a Postdoctoral Research Fellow at Karolinska Institutet, Sweden. He was then an Assistant Professor and Systems Microscopy Team Leader at Karolinska Institutet from 2010 to 2015. He is now Group Leader in Systems Microscopy of Cancer at the Faculty of Medicine of University of New South Wales, Sydney, Australia.

Hajar Moghadas is a PhD student of Mechanical Engineering at Sharif University of Technology, Tehran, Iran. She is interested in biomedical, cell culture and drug delivery researches, microchip fabrication and nano-micro particle mechanics. In particular, she works in lung cancer-on-a-chip. She received her B.Sc. degree, in Mechanical Engineering from Yasouj University, Iran, in 2005 (Ranked first among all entrance students in 2001). She graduated from Shiraz University, Iran, with an M.Sc in Mechanical Engineering (2009), with the award of top selected student.

Bahar Firoozabadi respectively obtained her BSc and MSc degrees in Mechanical Engineering from Sharif University of Technology and Tarbiat Modarres University, Tehran, Iran. In 1999, she received her PhD in Mechanical Engineering from Sharif University of Technology. She is now a Professor of Mechanical Engineering at Sharif University of Technology, Center of Excellence in Energy Conversion. Her research interests include: bio-fluid engineering, bubble and drop formation and motion and 3D microfluidic cell culture devices

Mohammad Said Saidi received his Master's and Ph.D. degrees from Massachusetts Institute of Technology (MIT). He is a Professor of Mechanical Engineering at Sharif University of Technology, Center of Excellence in Energy Conversion. He also serves as a director of Sharif Bioengineering Lab which is a multidisciplinary group focusing on biomedical applications of microfluidics from 3D cell cultures to organ-on-chips with especial interest on cancer modelling and drug screening. His research interest includes design and fabrication of microfluidic systems, experimental design and mathematical modeling of transport of nano and microscale aerosol particles, multiphase and reacting flow in porous media, micro and macro scale bioreactor.

Nam-Trung Nguyen is a professor and the director of Queens- land Micro- and Nanotechnology Centre, Griffith University, Australia. He received his Dipl-Ing, Dr-Ing and Dr-Ing habil degrees from the Chemnitz University of Technology, Germany, in 1993, 1997 and 2004, respectively. He was a postdoctoral research en- gineer at the Berkeley Sensor and Actuator Center, University of California, Berkeley, USA. From 1999 to 2013, he was a research fellow, assistant professor and associate professor at Nanyang Technological University, Singapore. Dr. Nguyen has published over 330 journal papers and several books on micro- fluidics and nanofluidics.

Table 1: The table summarizes the information discussed in sections 2 and 3.

Method of microfluidic spheroid formation	**Sub-types of the methods**	**Effecting parameters**
Emulsion technique [98-102, 105, 107]	Single (CS/O, Gel/O), double (CS/O/CM, CS/Gel/CM) and triple (CM/Gel/Gel/Oleic acid) emulsion	• Hydrogel type: The solid-like nature of the hydrogels might hinder spheroid formation • Droplet stabilization: adding surfactants improves droplet stability and spheroid formation • Flow rate: controls droplet generation frequency, droplet diameter and shell thickness • Droplet anchorage: prevents droplet coalescence. The anchorage sites might be microwells or sinusoidal shapes
U-shaped microstructures [18, 118, 121, 128]	Pneumatically actuated or permanent structures	• They can be used to trap both cells and cell containing droplets for spheroid formation. • The structure size controls the spheroid diameter. • The stagnation pressure in front of the structures facilitates spheroid formation. • The configuration of their location with respect to each other on-chip is crucial for proper trapping the cells or droplets.
Microwell-based [6, 39, 88, 96, 125, 134]	Sedimentation trapping or flow rate trapping	• Spheroid escape from the microwells can be predicted by CFD simulations and prevented. • The flow rate and cell paths through spheroid culture microchannels should be adjusted and equalized using hydraulic-electric analogy. • To facilitate HTS, the microchip should be designed such that it can be coupled with a CGG.
Other microfluidic methods [10, 54, 151-154]	Other methods used on-chip hanging droplets, permeable membranes, 3D acoustic tweezers, micropillars and microrotational flow for spheroid formation	• Porous membranes are used in two-layered chips for patterning the cells next to each other. • The microrotational flow design requires a large volume flow rate of culture medium. • The exposure time of cells within the on-chip 3D acoustic field is short, reducing cell death caused by

		sound waves. • The micropillars are used to minimize the direct exposure of spheroids to the flow-induced shear stress and confine the transport phenomena to diffusion. • On-chip hanging droplets have closed-loop steady and pulsatile culture medium flows for spheroid formation and culture. They still need adding culture medium to compensate for evaporation.
Microfluidic spheroid culture-only chips [8, 87, 89, 139]	Bypass microchannels, parallel narrow microchannels, cylindrical microstructures and microwells with square sections	• The design of μSCCs have the intended characteristics to facilitate the specific test on the spheroids. • The hydraulic-electric analogy is used to direct the spheroids towards the culturing sites on-chip. • Spheroids are used as the suitable 3D culture in some multi-organ-on-a-chip devices.
Digital microfluidics [173, 178]	This method uses HDs or hydrophilic sites on the chip for spheroid formation	• This method does not need any valves or pumps. • Droplet merging, mixing and splitting as well as dilution of solutions are possible on digital microfluidic chips. • Biofouling, liquid evaporation and lack of continuous perfusion are its deficiencies.